UNIVERSITY OF OKLAHOMA

GRADUATE COLLEGE

HEXANE CRACKING ON Y ZEOLITES: ACTIVITY ENHANCEMENT AND ITS POSSIBLE REASONS

A THESIS

SUBMITTED TO THE GRADUATE FACULTY

in partial fulfillment of the requirements for the

Degree of

MASTER OF SCIENCE

By

ANVIT VARTAK
Norman, Oklahoma
2016

HEXANE CRACKING ON Y ZEOLITES: ACTIVITY ENHANCEMENT AND ITS POSSIBLE REASONS

A THESIS APPROVED FOR THE
SCHOOL OF CHEMICAL, BIOLOGICAL AND MATERIALS ENGINEERING

BY

_____
Dr. Daniel Resasco, Chair

_____
Dr. Lance Lobban

_____
Dr. Steven Crossley

Dedication

To my Parents and my Brother.

Thank you for your love, support, encouragement and sacrifices.

Acknowledgements

I am very fortunate to have pursued my graduate college at University of Oklahoma; therefore, there are many people to thank for their part in my success. First and foremost, I would like to thank my advisor, ***Dr. Daniel Resasco***, for his guidance and support throughout my two years in graduate school, and especially for his confidence in me. Besides my research, he has also helped me in choosing graduate classes and ensured I was performing well. His comments and questions were very beneficial in my completion of the thesis manuscript. It was an honor to be a student with such a highly knowledgeable Professor and Research Advisor.

I would also like to thank my committee members, ***Dr. Lance Lobban*** *and* ***Dr. Steven Crossley***, along with ***Dr. Bin Wang*** for their contributions to this work. Over the course of two years, each has given me scientific guidance, many insightful suggestions and motivation towards gaining better knowledge in the field of my research. I am also grateful to ***Dr. Tawan Sooknoi*** for helping me with my project work and the constant motivation he provided me to obtain better results in this study.

I would like to thank Yen, Manasa, Abhishek, Rajiv, Dr. Lu Zhang, Dr. Xiang Wang and all the other friends in the biofuels group. Special thanks to *Yen Pham* and *Dr. Lu Zhang* whose previously conducted experiments have helped me a lot in this research. I would also like to thank the CBME Department and University of Oklahoma for giving me an opportunity to study and conduct research for these two years.

I would like to thank my parents for imbibing in me, good values and helping me in becoming the person I am now. A special thanks to my brother for keeping me in

touch with the sports world news whenever I was busy with studies or work. Their regular phone calls used to be entertaining as well as motivating.

I am thankful to all my friends at OU and elsewhere. My childhood friends Anoop, Ambarish, Pinak, Sandesh and Devang who have been and will keep building up memories forever. Disha, Chinmay, Shreya, Sunil, Aditi, Girish and Sidhant for being kind-hearted, humble and motivating. Tarek, Diken, Abhijeet, Soham, Maulin, Nauman, Harsh, Nidhi, Richa, Sumeer, Tabish, Fatema and many others who were always a part of a fun loving journey throughout the two years.

Table of Contents

List of Tables

List of Figures

Abstract

HY zeolites are an essential component as catalysts in fluidized catalytic cracking (FCC) process. The Steamed HY or Ultra Stable Y (USY) zeolites have proved to be active hydrocarbon cracking catalysts. Therefore, in this research we have conducted reactions for cracking of n-hexane on various HY zeolites (commercial and lab synthesized) which were prepared by steaming and/or acid leaching of the conventional HY zeolite. Catalytic cracking of n-hexane has been widely accepted as a probe for strong acidity in zeolites, and henceforth, it shall be a good measure of comparing activity differences in various HY zeolites.

The high activity of H-USY compared to HY has been previously explained by isolation of Brønsted Acid Sites (BAS) to create highly active BAS, or increased accessibility in a microporous diffusion-limited HY, or generation of Extra-framework Aluminum (EFAl) which greatly helps in the activity enhancement of HY zeolites. However, neither of the reasons have been proven to be fully correct and agreed upon by majority of the observations seen in literature. Therefore, properties of HY zeolites were studied using characterization methods like BET adsorption, ^{27}Al MAS NMR, ^{29}Si MAS NMR and IPA TPD. Calculated activation energies, reaction rates and turnover frequencies (TOF) were helpful in comparing the zeolites for any diffusion limitations or activity enhancements. After comparing activity of HY zeolites with HZSM-5, it was clear that the cracking of n-hexane over HY zeolites is not governed by diffusion of the reactant in terms of entering the pores of the HY zeolites. Cracking activity on various commercial HY zeolites was compared with quantified values of Framework Al (FAl) and EFAl. These comparisons helped in knowing that

isolated FAl might be a necessary, but insufficient condition for activity enhancement. Presence of EFAl might play a positive or a negative role in enhancing the activity. Furthermore, a comparison study of product distribution over a range of conversions between steamed HY and acid leached HY showed that longer diffusion paths inside the zeolite can lead to a large selectivity towards secondary reaction products formed from oligomerization and isomerization.

Chapter 1: Literature Review

1.1 Fluidized Catalytic Cracking (FCC)

Petroleum Crude Refining industry is one of the most important industries currently. Fluidized Catalytic Cracking (FCC) is a very important process in the refining industry for the production of gasoline among other products [1]. Gas oil is the primary feed for the FCC unit, which is a fraction of crude oil having a boiling point range of 330^{o}C to 550^{o}C [2]. FCC is a chemical process that uses heat and a catalyst to break down heavier components of gas oil into lighter and more useful products like diesel, gasoline and C4 gases like butane, butylene, isobutane and isobutylene. These products are in heavy demand particularly as transportation fuels and gasoline, making the growth of FCC, as the major petroleum refining process continues to grow at a rate of about 1.7% per year (1989-92) [3]. As of 2006, FCC units were in operation at 400 petroleum refineries worldwide and about one-third of the crude oil refined in those refineries is processed in an FCC to produce high-octane gasoline and fuel oils [42]. FCC units are more common in United States because of the high demand for gasoline, whereas Europe and Asia have a higher demand for diesel and kerosene which can be obtained through hydrocracking. Hence, US has a very high share of the world's FCC processing capacity.

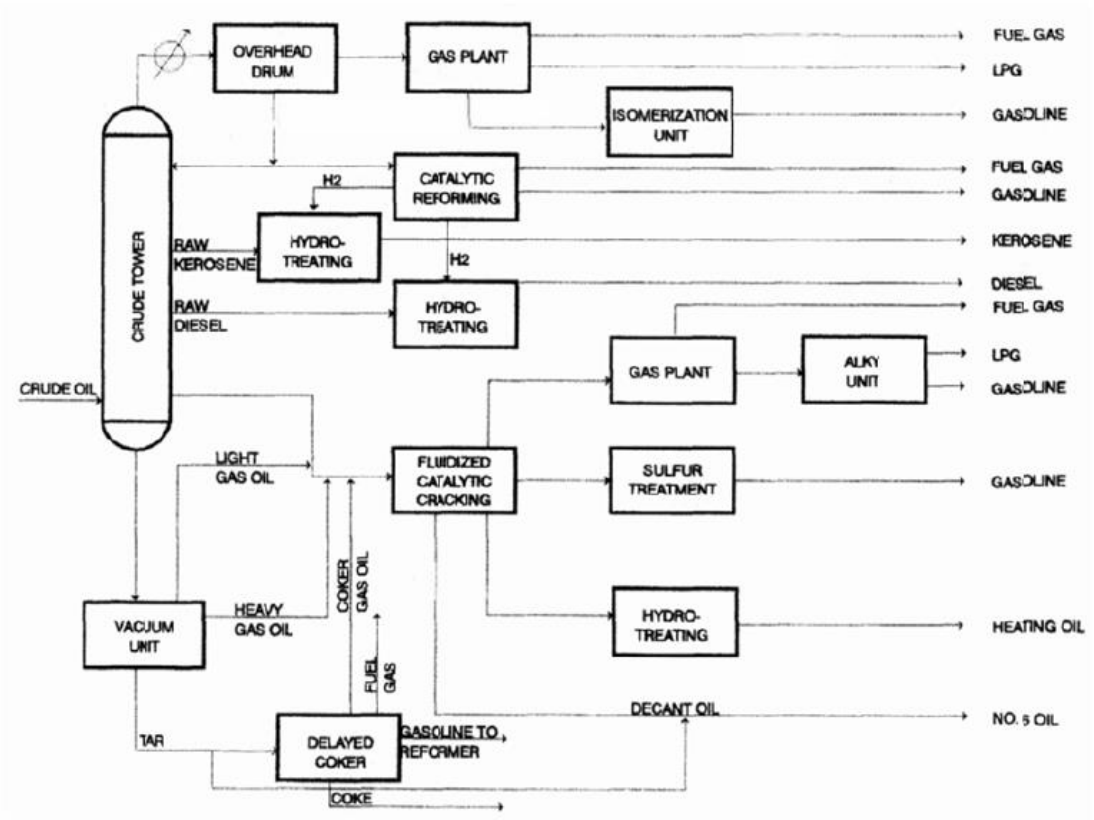

Figure 1. FCC Process Flow Chart [2]

1.2 Zeolites as FCC Catalysts

Catalysts are of prime importance in the FCC unit. The physical and chemical properties of the catalyst are largely influential in the design and operation of an FCC unit. The catalysts should have the following desirable properties: high activity, large pore size, good hydrothermal stability and low coke production. Zeolites are a very important active component of commercial FCC catalysts as they can easily satisfy the desired properties, after going through some modification processes. Matrix, binders and fillers are also used with zeolites in order to efficiently use the catalyst in the FCC unit. Zeolite content varies from about 15-50% of the catalyst as it is the primary active component. Zeolites are crystalline aluminosilicate materials with the composition

$M_{x/n}[(AlO_2)_x(SiO_2)_y]._zH_2O$. The cation M is a charge compensating alkali or alkali earth metal, with valency n. But, it can be exchanged with other metals or protons in order to achieve desired catalytic properties. Zeolites are microporous materials with tunable structure, acid density, and shape selectivity, which have shown unmatched performance in many vapor phase petrochemical and oil refining processes, including cracking, hydrocracking, isomerization, aromatization, etc. In the vapor phase, zeolites are reasonably stable under rather severe conditions (350−500 °C) [6].

1.2.1. Y Zeolites

The zeolite Y has a tetrahedral framework structure with Silica (Si) and Alumina (Al) as the elementary building blocks. The Al or Si atoms (T atoms) occupy the central position of the tetrahedron with four oxygen atoms at the corner. Each Oxygen atom is shared by two T atoms hence Si is neutral in charge because of its +4 Oxidation state and Al gets negatively charged because of its +3 oxidation state. This negative charge when balanced by a proton, gives rise to a Brønsted Acid Site (BAS) or leads to generation of a Lewis Acid Site (LAS) when other cations like Ca^{2+}, Li^{+}, Na^{+} balance the negative charge on Al [5].

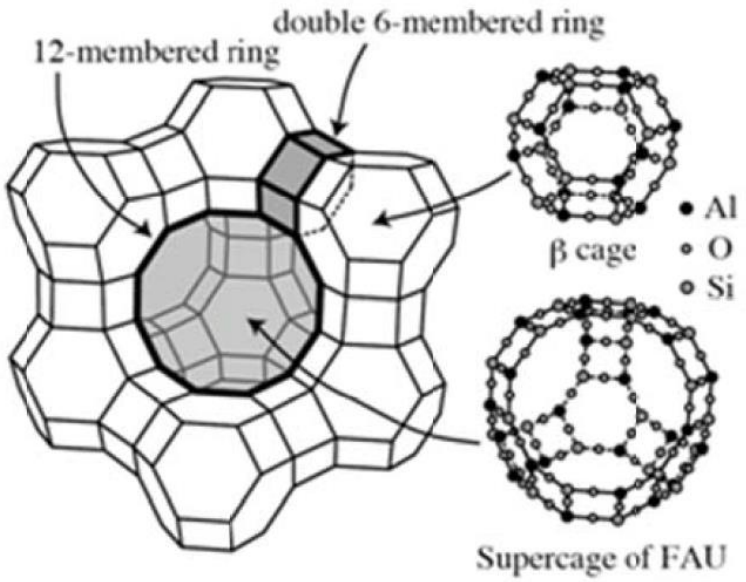

Figure 2a: Faujasite Y Zeolite Basic Structure [5]

Y Zeolite has a Faujasite structure (figure 2a) and its cubic unit cell consists of 192 T atoms per unit cell [5]. This Faujasite structure consists of two types of cages, which are the 12 membered supercage and the sodalite cage called as β-cage. Its pore system is relatively spacious with 1.3 nm diameter for the supercages connected tetrahedrally with four neighboring cages through windows with a diameter of 0.74 nm formed by 12 TO_4 – tetrahedra [6]. Hence, Y Zeolite is classified as a three-dimensional 12 membered ring pore system [6]. The connectivity of these cages allows the diffusion of molecules in three dimensions inside the crystal structure, making it favorable as a solid-acid catalyst in the FCC unit of a refinery [15].

1.2.2 ZSM-5 Zeolites

After Y zeolite, ZSM-5 is the second most used zeolite as the main catalytic component. ZSM-5 is used as a very important additive to enhance the octane number of gasoline fraction in an FCC unit. It also helps in reducing coke formation. The basic

building blocks of ZSM-5 are the 5-membered ring units. These rings are organized as columns and connected to each other in such a way that they form straight and sinusoidal channels with 10-membered ring windows (Figure 2b). These two channels only direct in two dimensions, but their interconnectivity allows the molecules to diffuse in three dimension inside the crystal.

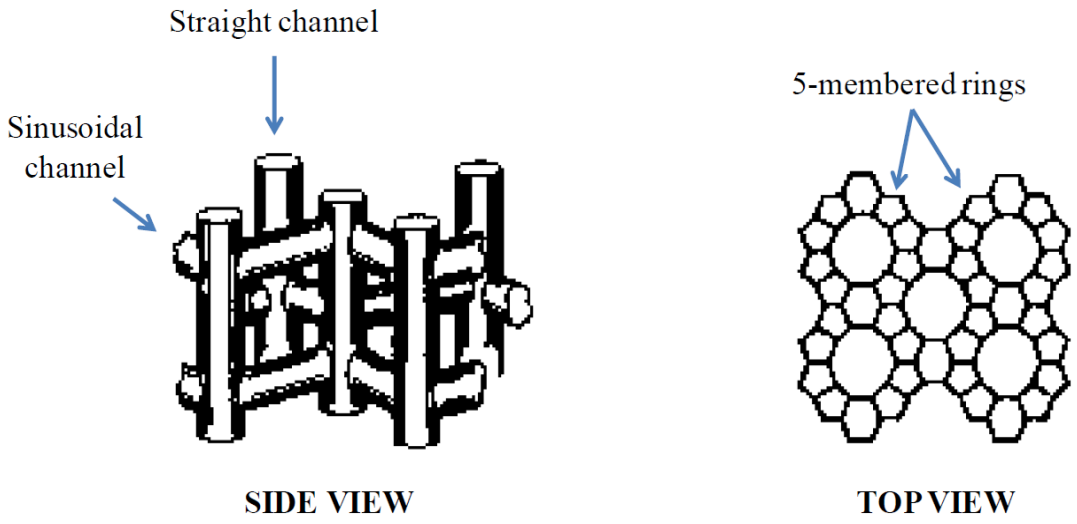

Figure 2b. ZSM-5 channel structure [46]

1.3 Dealumination: Synthesis of Ultra Stable Y (USY) Zeolite

1.3.1 Background

The Y Zeolites used in FCC undergo a regeneration process in the regenerator (figure 3), in order to burn off the deposited coke. This process takes place at very high temperatures, around 650-700^{o}C. The Y Zeolite is rich in Al as it can be directly synthesized with a maximum Si/Al ratio of 3. This Al rich environment is not stable for the zeolite at high temperatures and especially in the presence of water or steam. Dealumination occurs when the zeolite is exposed to water in vapor phase at high temperature [4]. The zeolite structure can be partially or even totally collapsed during

regeneration, where there is high amount of steam at temperatures around 677ºC - 732ºC. So, the zeolite has to be stabilized hydrothermally before using for FCC. A partial removal of Al through steaming can enhance its stability. Figure 3 below, shows the process flow for reaction and regeneration steps in FCC, along with temperatures for individual steps.

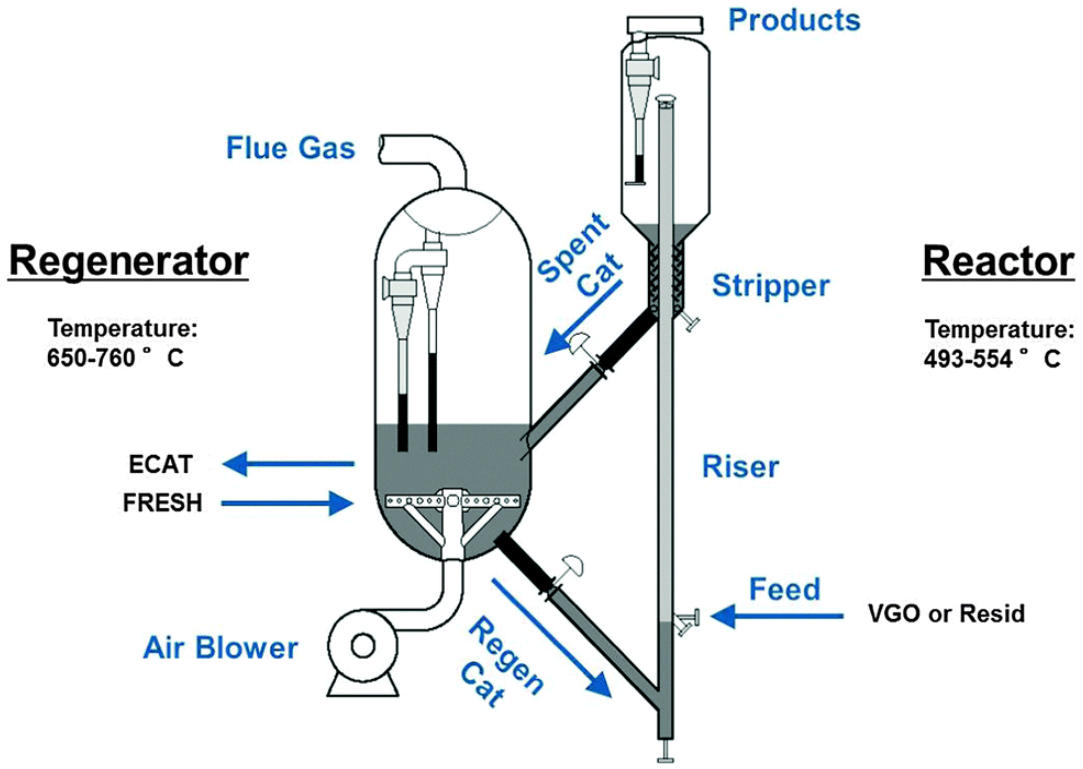

Figure 3: Diagrammatic representation of FCC Reactor and Regenerator [1]

1.3.2 Process of Dealumination

Thermal and chemical dealumination are the two major dealumination processes. Ultra Stable Y (USY) is the most used FCC catalyst currently. USY is a result of Thermal dealuminaton which is carried out by steam calcination of ammonium Y or HY zeolite at temperatures above 500ºC, with pressure of water less than or equal to 1 atm [16]. This causes a removal of Al from its framework tetrahedral position, and

leads to the formation of octahedral extraframework aluminum (EFAl). USY has a lower acidity (BAS density) and lesser framework Al, but shows a higher cracking activity along with better hydrothermal stability [7, 8]. Steaming also results in the formation of mesopores. A consequent increase in mesoporosity is again observed, when this steam dealuminated zeolite is further leached in presence of an acidic environment like HCl or Acetic Acid solution (figure 4). In chemical treatment, the zeolite is stirred with a solution of ammonium hexafluorosilicate (AHFS) or silicon tetrachloride ($SiCl_4$) which chemically extracts the framework Al and dissolves it the solution.

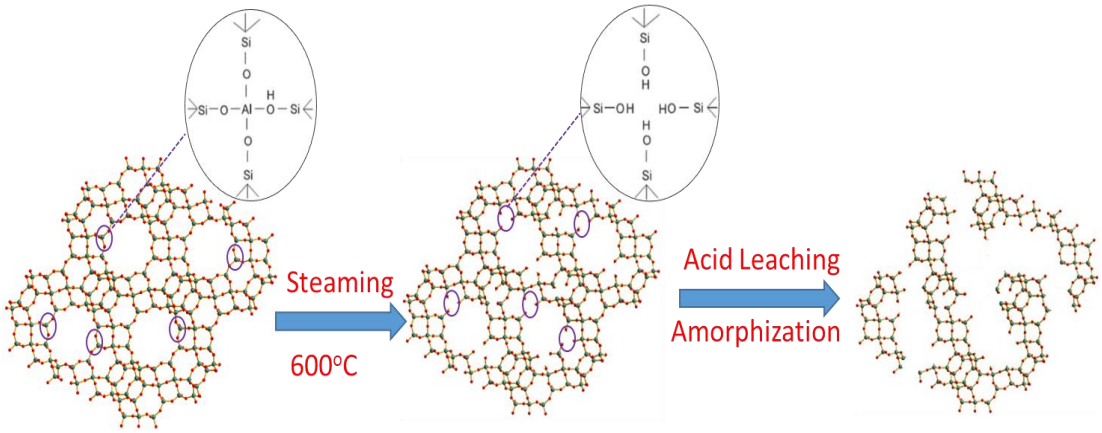

Figure 4. Formation of mesopores by steaming and acid leaching

The dealumination is generally a two-step procedure, which is customarily associated with the formation of framework defects called as hydroxyl nests [16]:
Step 1 – Water hydrolyzes Al to form Aluminum Hydroxide and four Silanol groups (figure 5). The Aluminum Hydroxide gets removed out of the framework and leaves back an Al vacancy.

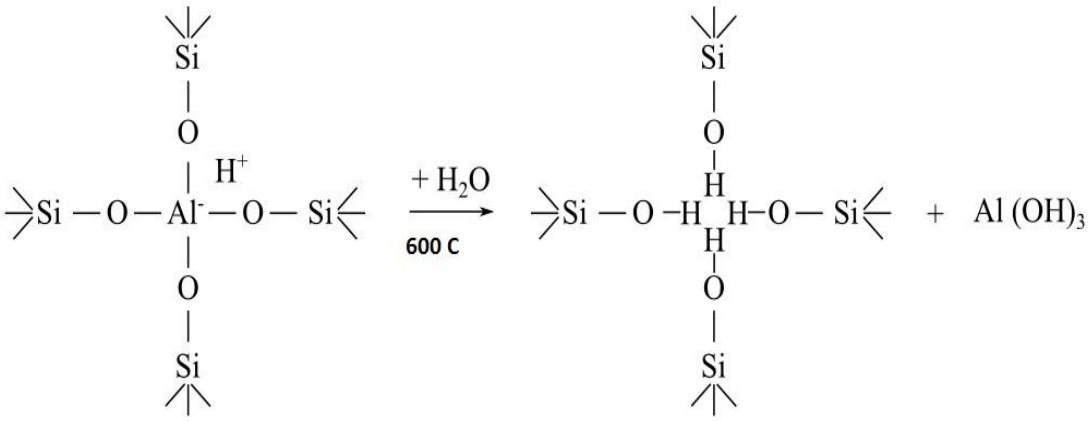

Figure 5. Dealumination Process – Removal of Al from framework position

Step 2 – The vacancy is filled by Si atom depending on the dealumination method used. If dealuminaton method is steaming or chemical leaching (extraction), the Si atom migrates from other collapsed section of the zeolite crystal, to fill the vacancy. There might be a limitation to the available number of Si atoms in the zeolite framework. In such cases where Si cannot fill in all the Al vacancies, four silanol groups interact through H-bonding to form a hydroxyl nest (figure 6) [17]. In case of chemical substitution, the vacancy can be filled in through the Si atom that is obtained from AHFS or $SiCl_4$.

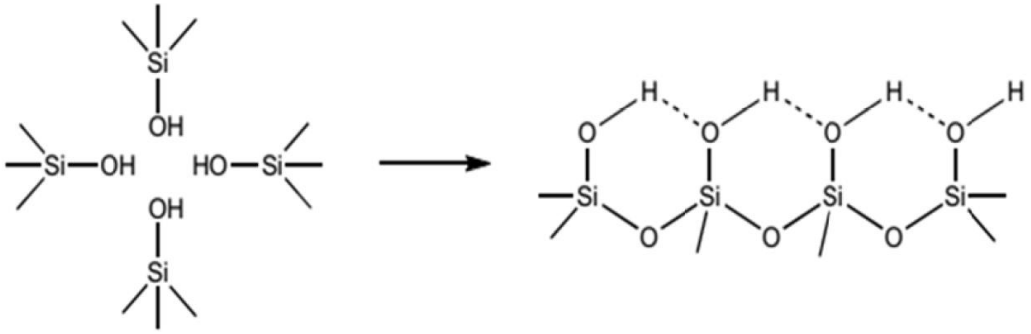

Figure 6. Formation of Hydroxyl nest defects

1.3.3 Extra-framework Aluminum (EFAl)

Different types of bulk defects are usually encountered within zeolites due to thermal or chemical dealumination, formation of hydroxyl nests and EFAl are the two most observed defects in zeolites. A variety of experimental techniques are used to analyze and characterize the local environment of Al, such as ^{27}Al MAS-NMR, X-Ray Diffraction (XRD), adsorption studies and IR. Unfortunately, none of these can single handed provide information about the location, nature and effect of the EFAl in specific manner. For example, MAS-NMR spectra can tell us the position of Al (tetrahedral, pentahedral or octahedral), but cannot provide the structure.

The various types of EFAl species that have been suggested in literature include neutral species like AlOOH and $Al(OH)_3$), oxoaluminum cations like AlO^+, $Al(OH)^{2+}$ and $AlOH^{2+}$; or they might be alumina clusters having boehmite-type topology which is very similar to γ-AlOOH [18]. The amount of EFAl and its position is a very important factor in knowing if EFAl helps in activity enhancement. Steam dealumination generates a high amount of EFAl as the Al resides in octahedral positions after being removed from the tetrahedral positions [7], but chemical treatment with ammonium hexafluorosilicate (AHFS) can synthesize Y zeolites with no EFAl as the FAl gets dissolved in the AHFS solution after being removed from the framework tetrahedral position [8].

1.3.4 Interaction between EFAl and BAS

There is evidence in the literature about the activity promoting effects of EFAl species present in the faujasite Y. But, the understanding of the mechanisms in which it happens or the exact nature of EFAl which affects activity hasn't been understood totally. In a study done by Beyerlein and co-workers [8], they compared conversion for isobutane between AHFS dealuminated Y and USY having a similar number of FAl (where USY importantly had a large amount of EFAl). A very low isobutane conversion was observed on AHFS dealuminated Y. The introduction of EFAl into the AHFS dealuminated Y drastically improved the conversion as well as carbonium ion selectivity, which was found to be even higher than USY [8]. This suggested an important role of EFAl in activity enhancement. The lesser amount of EFAl in AHFS dealuminated Y also meant that having an optimum number of EFAl is important for maximum activity. Three mainstream hypothesis found in literature that explain the favorable effect of EFAl [41] are: (i) some EFAl themselves are Lewis acid sites [32]. (ii) the EFAl species stabilize the charges on the lattice after the removal of acidic proton [40]. (iii) there is synergistic effect between EFAl and nearby BAS [33, 34, 35]. Out of these three, charge stabilization and the existence of BAS EFAl synergism is very actively debated in the literature.

Mirodatos et al. [33] presented a concept of direct interaction between EFAl (acting as LAS) and the oxygen connected to the acidic proton. A partial electron transfer from oxygen to EFAl would take place, which would weaken the O-H bond strength, hence increasing the acid strength of the site. Mota et al. initially disagreed with the hypothesis, saying that DFT calculations showed a decrease in acid strength for

a direct interaction between EFAl and BAS attached oxygen. Furthermore, Mota et. al compared the stability of different types of mononuclear EFAls interacting with a T6 cluster model of a zeolite using DFT calculations and identified that $[Al(OH)]^{2+}$ was a preferred structure for the monovalent cations such as AlO^{+} [40]. The proposed reason for this was that the interaction of such a cation with a vicinal BAS leads to enhanced acid strength by stabilizing the conjugated base site at the zeolite lattice via hydrogen bonding. The results of ^{1}H MAS NMR studies conducted by Li et al. [41] also agreed with the concept that instead of a direct interaction with OH group of BAS, EFAl might co-ordinate with the next immediate oxygen atom of BAS, in order to increase acid strength. Scheme 1 (reprinted from [41]), shows both proposals with the former one by Mirodatos et al. and the latter by Li et al.

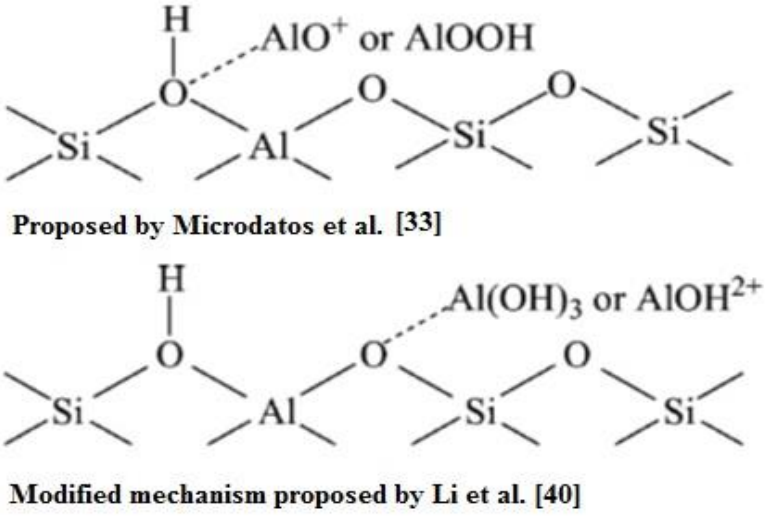

Scheme 1. Comparison of mechanisms for EFAl-BAS interaction to increase acid strength. Reprinted as depicted in [40]

1.4 Pathways for cracking of n-hexane over Zeolites

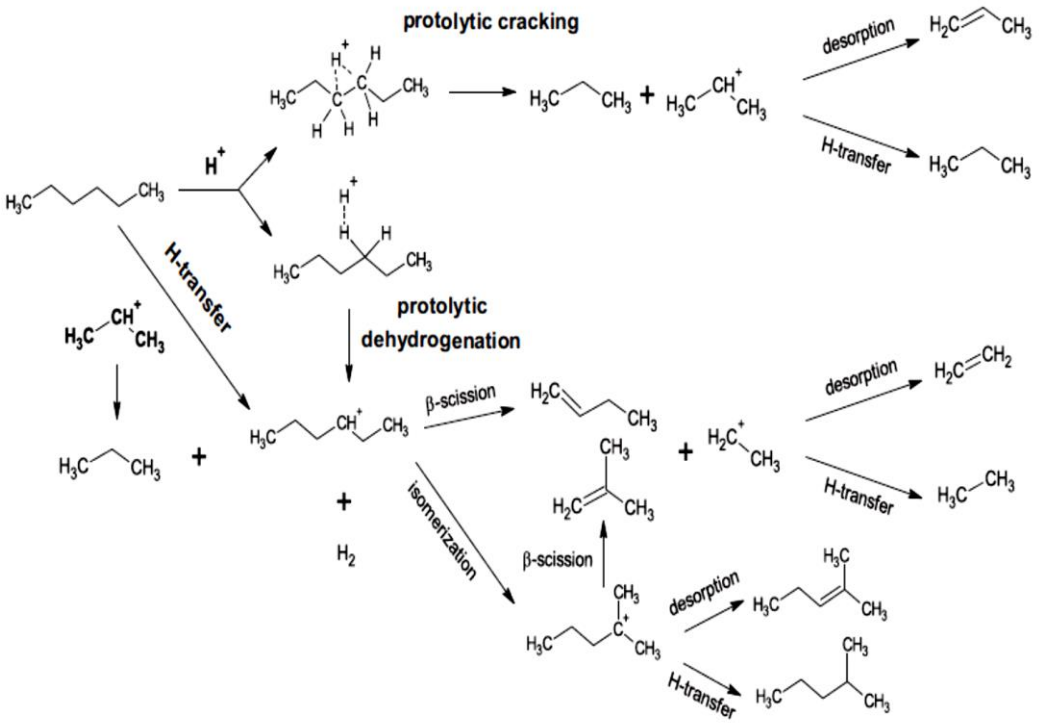

Scheme 2. Reaction pathways for n-hexane cracking over zeolite [11]

The catalytic cracking of hydrocarbons over zeolites is one of the most important chemical reactions involved in the refining of crude oil for the production of fuels and chemicals. Depending on the reaction conditions, cracking may occur via bimolecular or monomolecular pathways. Resasco et al. mention the most widely accepted pathways proposed in literature as [11]: (i) protolytic cracking of C–C bond in the penta-coordinated carbonium ion, protonation of the paraffin by H+ of BAS, (ii) protolytic dehydrogenation of the carbonium ion, and (iii) hydride transfer with a surface carbenium ion. The first two pathways are monomolecular reactions that occur on BAS, whereas the third pathway involves a carbenium ion in transition state. Besides hydride transfer with paraffinic feed (as described by (iii) route), other reactions involving the participation of carbenium ions include isomerization, β-scission, and

desorption to regenerate the BAS [11]. The pictographic depiction of the various pathways has been shown in Scheme 2.

In conversion of alkanes over zeolites, the monomolecular and bimolecular pathways always co-exist and compete with each other; their contribution varies depending on reactions conditions [19,20].

1.5 Research Objectives

- The various characterization of different commercial HY zeolites showed a significant difference due to dealumination methods. By comparing cracking activity of n-hexane over various zeolites, the effect of dealumination can be studied.
- Through this study, we aim to know whether or not, diffusion limitations exist in HY zeolites which might hinder the activity for n-hexane cracking. Arrhenius plots for n-hexane cracking over commercial HY zeolites were plotted to calculate activation energy barriers. Multiple experiments were conducted to investigate the presence of diffusion limitations in HY zeolites.
- Extra-framework Aluminum (EFAl) is obtained because of dealumination of zeolites. Understanding the effect of this EFAl on activity is very important. Removal of EFAl can be done by acid leaching of commercial zeolites. Performing reactions and characterization for HCl and Acetic Acid leached commercial HY zeolites would help in knowing about the role of EFAl in cracking activity of HY zeolites. Results from these experiments were used to study the role of EFAl in activity enhancement.

Chapter 2: Experimental

2.1 Materials – Reactant and Catalyst Preparation

Two C_6 alkanes were used in this study: n-Hexane (n-C6, 99% pure) from Sigma Aldrich and 2,3 – dimethylbutane (2,3 – DMB, 99%+) from Tokyo Chemicals Inc. These hydrocarbons were used for the reaction through direct injection via syringe pump, without further purification or treatment.

Five commercial Y zeolites and one ZSM-5 zeolite were obtained from Zeolyst International. The Y zeolites are CBV300 (HY2.6NS), CBV600 (HY2.6St), CBV720 (HY15), CBV760 (HY30), CBV 780 (HY40); and ZSM-5 is CBV8014. Table 1 shows the basic properties of the commercial zeolites, as mentioned on the company website.

Table 1. Properties of Commercial Zeolites as mentioned on manufacturer's website

Zeolites	Total Si/Al Ratio	Nominal Cation Form	Na_2O Wt. %
CBV300 (HY2.6NS)	2.55	Ammonium	2.80
CBV600 (HY2.6St)	2.6	Hydrogen	0.20
CBV720 (HY15)	15	Hydrogen	0.03
CBV760 (HY30)	30	Hydrogen	0.03
CBV780 (HY40)	40	Hydrogen	0.03
CBV8014 (HZSM-5)	40	Ammonium	0.05

The commercial CBV300 (HY2.6NS) is obtained in the ammonium form, but it is important to have BAS for the zeolite to be active for cracking reactions. Hence, it is calcined to obtain H-form of CBV300 (HY2.6NS). First, it is dried at 110^{o}C overnight,

in flowing Helium (30 mL/min). For the second step, temperature is raised from 110°C to 550°C at 5°C/min and the catalyst is calcined at 550°C for 3 hours. This step results in the removal of ammonia and leaves back a proton which forms the BAS. To achieve close to 100% H-form, the calcination can be repeated twice (the process is followed as prescribed by our Post Doc., Dr. Lu Zhang).

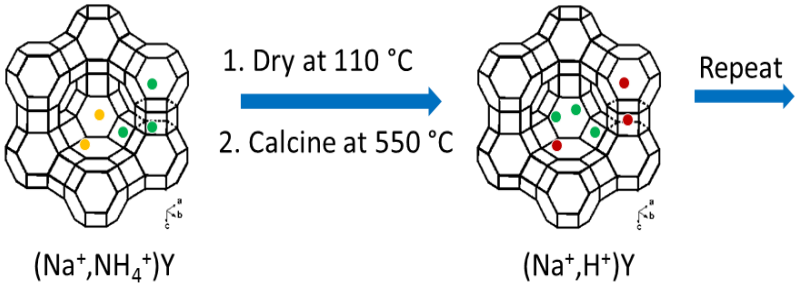

Figure 7. Ion exchange process to obtain Proton (H^+) form of CBV300

CBV600 (HY2.6St) is obtained by steaming the parent CBV300 (HY2.6NS) at 600°C [21]. CBV720 (HY15) and CBV760 (HY30) were formed by mild acid leaching of CBV600 (HY2.6St). Whereas, a second steam treatment at higher temperature followed by mineral acid leaching gives CBV 780 (HY40) [21].

Acid leaching of CBV300 (HY2.6NS), CBV600 (HY2.6St) and CBV760 (HY30) was performed by using 0.2M HCl to attack the zeolites at 80°C. 1 gm zeolite powder was mixed with 30 mL of 0.2M HCl solution and stirred at 350 rpm. The exchange occurred for 6 hours and temperature was kept constant at 80°C. The exchanged zeolite was centrifuged and washed 6-7 times with deionized (DI) water. The catalyst was then dried at 120°C for 24 hours, in vacuum. These catalysts were labelled as 0.2MHCl-CBV300, 0.2MHCl-CBV600 and 0.2MHCl-CBV760. A similar synthesis procedure was used to attack the parent zeolites with 3M Acetic Acid at 65°C.

CBV300 was exchanged with Na^+ cations by stirring in an aqueous 0.1M $NaNO_3$ at room temperature. The ratio of mL solution/gm catalyst was kept constant at 20. The exchange occurred for 10 hours. The exchanged zeolite was centrifuged and washed 6-7 times with DI water. The catalyst was kept at 110^{o}C in the oven to dry overnight. It was labelled as Na-CBV300.

All the catalysts were pelletized to particles of size range 90-250 μm before using for reaction.

2.2 Catalyst Charaterization

The ratios of framework Si to framework Al were calculated using ^{29}Si MAS NMR results. The number of framework Al (FAl) and extraframework Al (EFAl) were estimated by ^{29}Si MAS NMR using the reported method [22] (used by Dr. Lu Zhang in her calculations) and by XRD using the method developed and reported by Sohn et al. [23]. All XRD experiments were conducted by the Geology Department at University of Oklahoma. All ^{29}Si MAS NMR and ^{27}AL MAS NMR spectra were obtained from Florida State University.

The micropore and mesopore volume results were obtained from Nitrogen Adsorption Method by BET analysis performed on all the used commercial Y zeolites and lab synthesized acid leached HY zeolites. Thanks to Dr. Lu Zhang and Dr. Xiang Wang for performing these experiments.

The Brønsted acid sites (BAS) density was quantified by temperature-programmed desorption (TPD) of adsorbed isopropylamine (IPA). 50 mg of catalyst was pretreated at the same conditions employed before the reaction. After pretreatment,

the temperature was cooled down to 100^{o}C, and the flow of Helium was also reduced to 20 ml/min. 10 injections of IPA (2-3 μL/ injection) were performed. After 3 to 4 hours of flushing catalyst under He to remove weakly adsorbed IPA, the temperature was increased from 100^{o}C to 600^{o}C (10^{o}C/ min) to catalyze the reaction of IPA. The desorbed products were analyzed on a Microvision Plus MS, scanning over a 1- 60m/z range at a speed of 26 cycles/min. The amount of BAS is calibrated based on pulsing a known amount of propylene (100 μL).

2.3 Catalytic Measurements

The conversion of n-Hexane and 2,3 – dimethylbutane (2,3 – DMB) on HY zeolites was carried out in a flow reactor, with N_2 carrier gas at an atmospheric pressure. Catalysts pellets in the range of 90-250 μm were mixed with acid washed glass beads (150-220 μm) and packed between two layers of glass wool, in a 1/4th inch diameter quartz tube reactor. All zeolites were pretreated at the specific reaction temperature for two hours in 30 mL/min of flowing N_2 before undergoing any reactions. The reactants were fed through syringe pump. The products were analyzed online by using HP7890 Gas Chromatograph (GC), equipped with an HP-PLOT/Al2O3/"S" column and a Flame Ionization Detector (FID) which was directly connected to the reactor outlet. The pulses given to GC were controlled by using a six-port valve having a 100 μL sample loop.

Chapter 3: Results and Discussion

3.1 Catalyst Characterization

A wide range of catalyst characterization has been already done by Dr. Lu Zhang and Yen Pham, for most of the commercial HY zeolites used in this study. All of the results would be very helpful in discussing about the activity results for C_6 cracking on HY zeolites. Hence, it would be very important to understand those results to have an idea about the catalysts that are to be compared.

3.1.1 ^{27}Al MAS NMR and ^{29}Si MAS NMR

Figure 8 shows the ^{27}Al and ^{29}Si MAS NMR spectra of all the commercial HY zeolites having different total Si/Al ratios. In ^{27}Al MAS NMR spectra peaks occurring at 0, 30 and 60 ppm designate Al in Octahedral EFAl, Distorted Tetrahedral EFAl (or Pentahedral EFAl) and Tetrahedral FAl positions respectively. The FAl per unit cell and EFAl per unit cell values can be calculated from these signals combined with ICP measurements, as mentioned in table 2 (calculations done by Yen Pham). According to Figure 8, at least some Octahedral EFAl is observed in all the zeolites, but only CBV600 (HY2.6St) has a clearly visible Pentahedral or Distorted Tetrahedral EFAl peak at 30 ppm. A broader and larger signal at 0 ppm is an indication of a very high number of Octahedral EFAl with many different types of EFAl species in close proximity with each other. The ^{27}Al MAS NMR signal gets broadened with increasing interactions of EFAl with its surrounding atoms. CBV600 (HY2.6St) undergoes steam treatment at 600^{o}C in a water vapor environment that causes successive removal of a high amount FAl, which further rearranges itself in Octahedral EFAl or Pentahedral

EFAl positions. Mild Acid leaching of CBV600 (HY2.6St) produces CBV720 (HY15) and CBV760 (HY30). It helps in leaching some amount of EFAl, but also removes some FAl present in CBV600 (HY2.6St). It can also be seen from the BAS density and FAl/uc values given in Table 2. A second steam treatment at higher temperature followed by mineral acid leaching of CBV600 (HY2.6St) produces CBV780 (HY40). Hence, CBV780 (HY40) has a substantially collapsed structure.

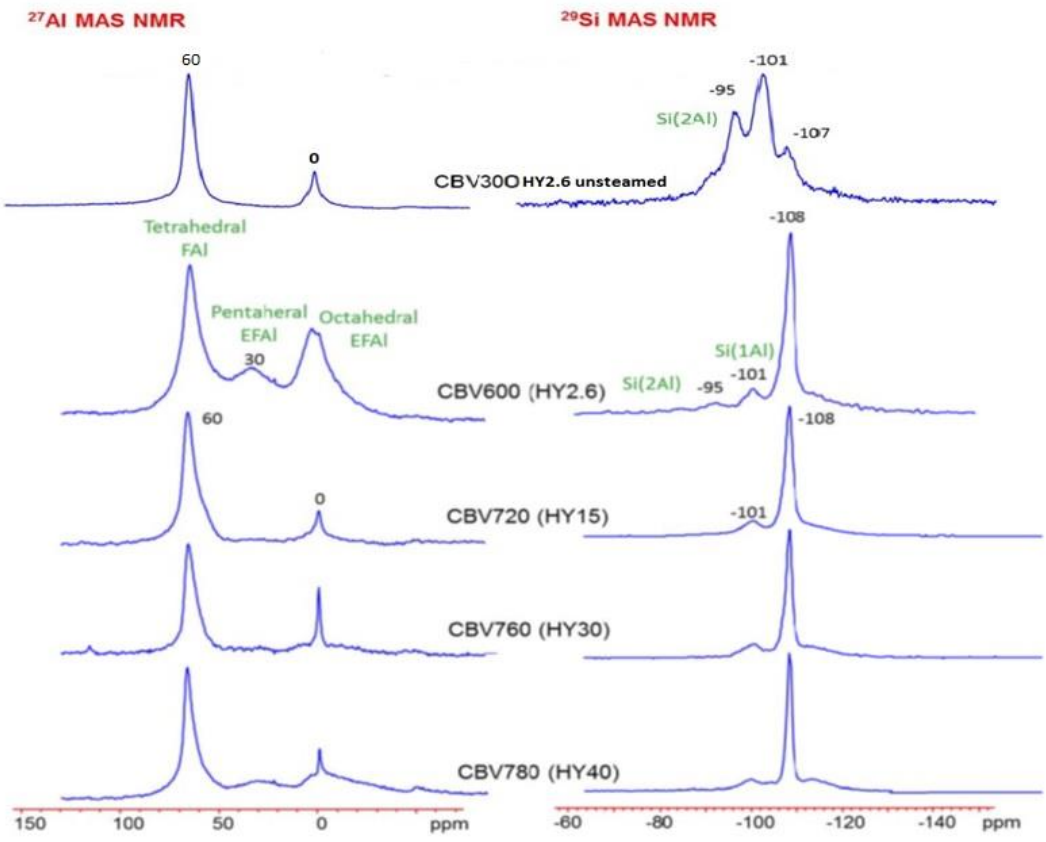

Figure 8. ^{27}Al MAS NMR and ^{29}Si MAS NMR of commercial HY Zeolites

^{29}Si MAS NMR helps in knowing the number of FAl atoms connected to every Si atom. The peaks at about -85, -90, -95, -100 and -105 represent Si atoms that are connected to 4, 3, 2, 1 and 0 FAl atoms, respectively. In figure 8, they are labelled as Si(4Al), Si(3Al), Si(2Al), Si(1Al) and Si(0Al). CBV300 has signals for Si(0Al), Si(1Al) as well as Si(2Al); which is justified because it has a very high FAl/uc value (Table 2). CBV300 (HY2.6NS) is known to be in crystalline form whereas the other zeolites start losing crystallinity because of increasing dealumination due to steaming and acid leaching. Rest of the commercial zeolites have very large Si(0Al) signal, with a low but noticeable Si(1Al) signal. CBV600 (HY2.6St) shows a peak for Si(2Al) which might be because it still has a comparatively high FAl/uc value compared to acid leached commercial zeolites.

Table 2. Characteristic Properties of Zeolites

Zeolites	Total Si/Al[a]	F(Si/Al)[b]	FAl/uc[b]	FAl/uc[d]	EFAl/uc[b]	BAS density (mmol/gm)[c]
CBV300 (HY2.6NS)	2.55	-	-	50.1	-	0.998
CBV600 (HY2.6St)	2.6	14.64	12.3	13.4	52.6	0.48
CBV720 (HY15)	15	37.24	5.0	-	6.5	0.356
CBV760 (HY30)	30	41.99	4.5	-	2.2	0.257
CBV780 (HY40)	40	50.26	3.7	-	1.0	0.09

a – Reported by Manufacturer

b – Estimated from ^{29}Si MAS NMR (Reported by Yen Pham)

c – Quantified by IPA TPD

d – Estimated from unit cell size obtained from XRD (Reported by Yen Pham)

3.2.2 BET Analysis

Table 3. Micropore and Mesopore Volume by BET Analysis

Catalyst	[a]Bulk Si/Al	[b] BAS Density (mmol/gm.cat)	[c] V_{micro} (cm^3/gm)	[d] V_{meso} (cm^3/gm)
CBV300 (HY2.6NS)	2.55	0.998	0.329	0.023
CBV600 (HY2.6St)	2.6	0.48	0.279	0.136
CBV760 (HY30)	30	0.257	0.358	0.211

a – As reported by manufacturer

b – Measured by IPA TPD

c and d - BET Analysis

Table 3 shows values obtained from BET analysis. By comparing values in the table, we see an increasing trend in the mesopore volume. We know that high amount of FAl gets removed when CBV300 (HY2.6NS) is steam treated to form CBV600 (HY2.6St). This creates defects in the zeolite structure which starts collapsing the structure, and creates mesopores. One major reason for the micropore volume going down in the case of CBV600 (HY2.6St) can be the presence of pentahedral or distorted EFAl. This EFAl might be blocking the micropores, and hence making it difficult for the probe molecules to enter micropores and detect them. Mild acid leaching of CBV600 (HY2.6St) removes some FAl along with some EFAl. More FAl removal will form more mesopores and also cause a high loss of crystallinity to form an amorphous CBV760 (HY30). On the other hand, removal of EFAl will open the plugged micropores and improve accessibility for the probe molecule to detect micropores.

3.2 Activation Energy Calculations

The catalytic cracking of n-hexane proceeded without any major deactivation on the commercial HY zeolites during a 5-hour reaction period. Even minor deactivation was taken into consideration by extrapolating the conversion on all catalysts to time t = 0. The apparent activation energies for CBV300 (HY2.6NS), CBV600 (HY2.6St) and CBV760 (HY30) were calculated from the slopes of the Arrhenius plots in Figure 10. The calculated values are listed in Table 4. These three commercial catalysts were selected because they showed considerable differences in their characteristics due to the methods of synthesis.

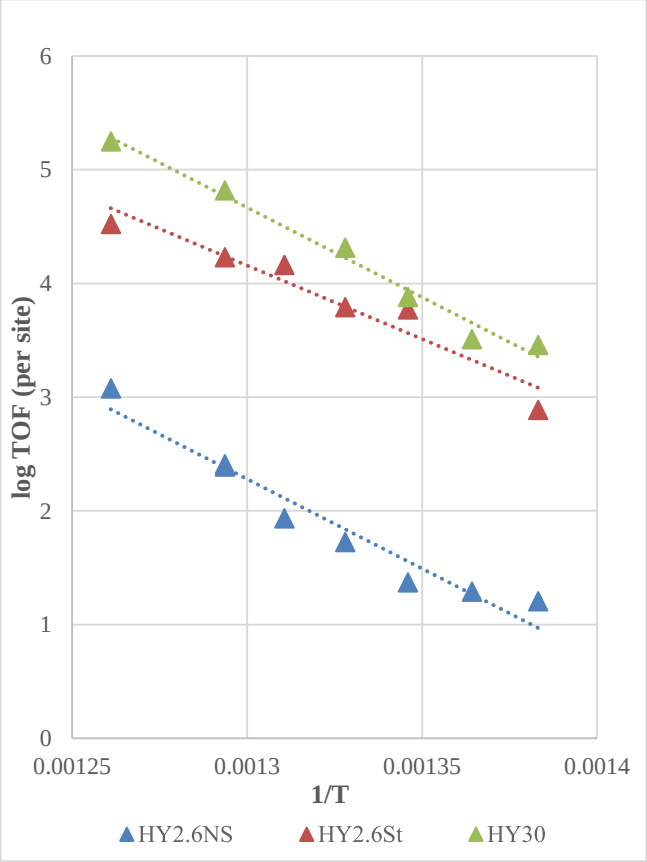

Figure 10a. Arrhenius Plots for n-hexane cracking over HY zeolites

The apparent activation energies (E_{app}) for CBV300 (HY2.6NS) and CBV760 (HY30) are similar, but a comparatively low E_{app} is observed in the case of CBV600 (HY2.6St). The possible reasons for this are discussed in the further sections of this study.

Table 4. Apparent Activation Energies for commercial HY Zeolites

Catalyst	BAS Density (mmol/gm.cat)	Activation Energy (E_{app})	
		kcal/mol	kJ/mol
CBV300 (HY2.6NS)	0.998	31.3	130.8
CBV600 (HY2.6St)	0.48	24.1	100.7
CBV760 (HY30)	0.257	31.4	131.2

3.3 Cracking Activity Comparison

From Table 2 and Table 3, we notice the major differences in BAS density, FAl/uc and EFAl/uc of CBV300 (HY2.6NS), CBV600 (HY2.6St) and CBV760 (HY30). Hence comparing the activity on these three zeolites will give us a good indication of how difference in synthesis methods could lead to changing activities.

Table 5. Activity Comparison Chart

Zeolite	Weight (mg)	BAS Density (mmol/gm catalyst)[a]	TOF (hr^{-1})	Rate (mol/hr-gm)	Conversion
CBV300 (HY2.6NS)	50	0.998	3.83 [3.2][b]	0.0033	5.49 [4.87][c]
CBV600 (HY2.6St)	50	0.48	19.5 [17.9]	0.0086	13.56[12.59]
CBV760 (HY30)	50	0.257	35.51 [33]	0.0086	13.4 [12.7]

a – Quantified by IPA TPD experiment

b and c – Values in brackets are values for TOF Cracking and Cracking Conversion, respectively

All the experiments in Table 5 were done at 450^{o}C after preheating the zeolites at 450^{o}C for two hours. The rate of reaction was calculated using cracking conversions given in brackets. Conversions were extrapolated to time t = 0 after 5 hours of reaction. The calculations are as follows:

1. Turnover frequency = $(X * F_{A0}) / (W * \text{BAS density})$

   where, X = Cracking Conversion of Hexane

   F_{A0} = Feed rate of Hexane = $3.0419 * 10^{-3}$ mol/hour

   W = Weight of catalyst in grams

2. Rate = $(F_{A0} * X) / W$
3. TOF Cracking = F_{A0} * (total yield - yield of C6 isomers) / (W * BAS density)

According to the cracking mechanism known commonly from literature, we know that protonation of a C-C bond in the hydrocarbon is the initiation step for cracking [24, 25]. To protonate, a proton (H^{+}) is needed and hence the zeolite with maximum BAS should exhibit highest activity. But, from Table 5, we can see that the unsteamed CBV300 (HY2.6NS) has a very low rate compared to CBV600 (HY2.6St) and CBV760 (HY30), which are steamed and acid leached respectively. Hence, it is not just the BAS density that is influencing in the cracking. Some other possible reasons could be: (1) Diffusion Limitation – CBV300 (HY2.6NS) does not have much mesopores as it is highly crystalline. The high microporosity makes diffusion of reactants difficult to make diffusion the rate limiting step. (2) the TOF increases as the BAS density goes on decreasing. Having more FAl means having more next nearest neighbor (NNN) Al atoms.

These NNN atoms can have electronic effects, which might lower the strength of BAS in CBV300 (HY2.6NS). Therefore, CBV300 (HY2.6NS) has lower TOF compared to CBV600 (HY2.6St) and CBV760 (HY30). (3) CBV600 has a lot of EFAl, which can block the diffusion pathway of hexane and result in a lower TOF. So, the TOF increases in case of CBV760 (HY30), when the EFAl is removed. (4) the penta-coordinated EFAl and octahedral EFAl might be having different effects on the activity enhancement, with one affecting positively while the other having a negative effect. In this study, we will try to investigate each of the possible reasons.

3.4 Diffusion Limitation Study

The overall process by which heterogeneous catalytic reactions proceed can be broken down into the sequence of individual steps shown in Scheme 3. The steps are as follow [44]:

1. Mass transfer (diffusion) of the reactant (example – species A) from the bulk fluid to the external surface of the catalyst pellet.
2. Diffusion of the reactant from the pore mouth through the catalyst pores to the immediate vicinity of the internal catalytic surface.
3. Adsorption of reactant A onto the catalyst surface.
4. Reaction on the surface of the catalyst (A → B)
5. Desorption of the products (e.g. B) from surface.
6. Diffusion of the products from the interior of the pellet to the pore mouth at the external surface.
7. Mass transfer of the products from the external pellet surface to the bulk fluid.

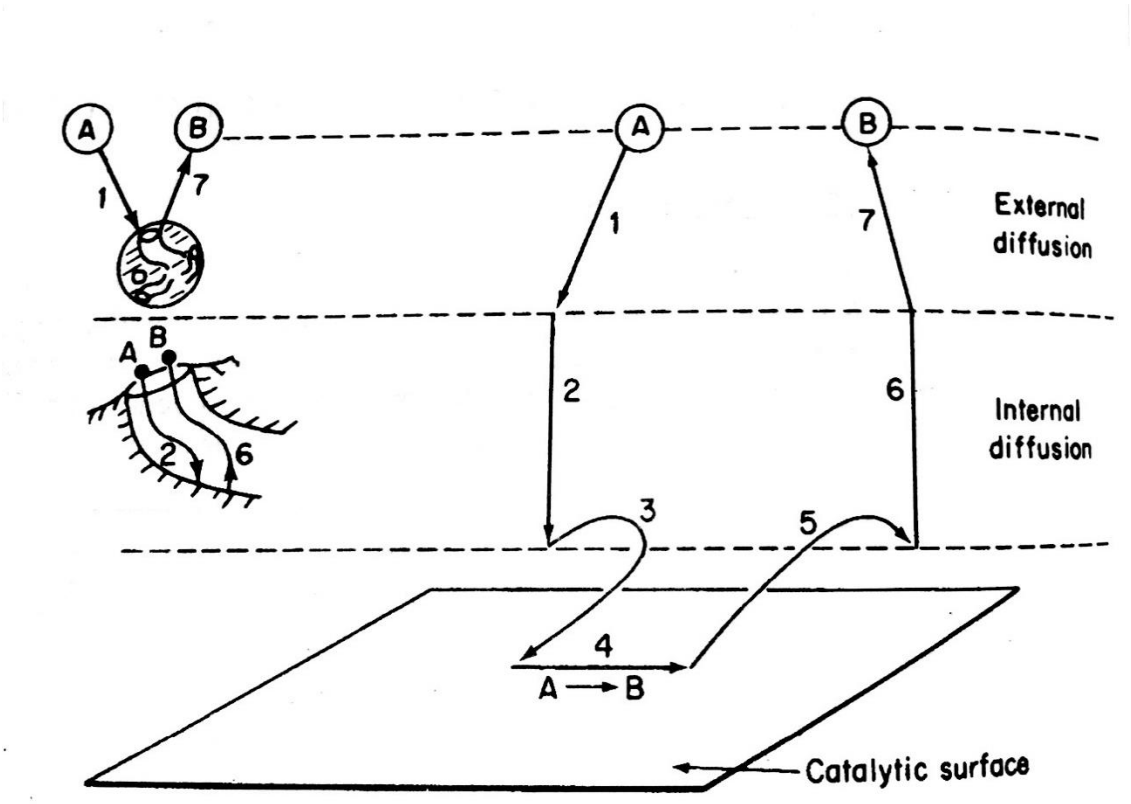

Scheme 3. Steps in a heterogeneous catalytic reaction [44]

When steps (1, 2, 6 and 7) are very fast compared with the reaction steps (3, 4 and 5), the transport or diffusion steps do not affect the overall reaction rate. In other situations, if the reaction steps are very fast compared with diffusion steps, mass transfer does affect the reaction rate.

Steps 1 and 7 – Diffusion from bulk to the external surface of the catalyst: All the resistance to mass transfer from bulk to the surface of catalyst is lumped together in the boundary layer surrounding the pellet. The rate constant is inversely proportional to the boundary layer thickness δ and depends directly on the diffusivity D_{AB} given as:

$$k_C = D_{AB} / \delta.$$

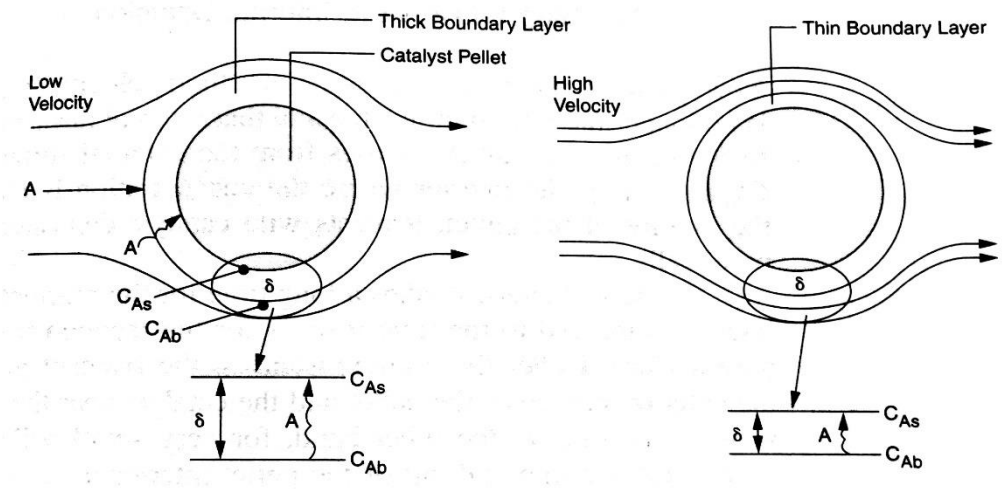

Scheme 4. Diffusion through the external boundary layer [44]

In the case of our vapor phase reactions in a flow reactor, the boundary layer thickness is very small because of high turbulence due to very high gas velocities. Hence, the overall reaction rate is unlikely to be affected by external mass transfer in this study.

Steps 2 and 6 – Internal diffusion through the pore system:

Thiele modulus – Thiele modulus quantifies the ratio of reaction rate to the diffusion rate in a pellet. When the Thiele modulus is large, internal diffusion usually limits the overall rate of reaction; when it is small, surface reaction is usually rate-limiting.

$$\phi_n^2 = \frac{k_n R^2 C_{\mathrm{As}}^{n-1}}{D_{\mathrm{e}}} = \frac{\text{“a” surface reaction rate}}{\text{“a” diffusion rate}}$$

In this section, we explore all different possibilities in which CBV300 (HY2.6NS) or CBV600 (HY2.6St) could be diffusion limited. For example, reducing the number of BAS (per gram) in a particular catalyst should reduce the per gram reaction rate. On the other hand, if the reaction rate is limited by internal diffusion, the

reaction rate values will be similar (Figure 10b) as most of the reaction is suspected to take place on the surface near the pore mouth in the catalyst pellet.

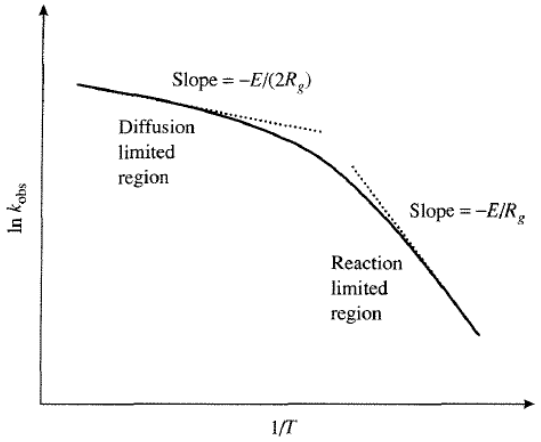

Figure 10b. Diffusion limited and reaction limited regions in Arrhenius plot [45]

3.*4.1 Sodium Exchange*

During Sodium exchange, the BAS sites get deactivated because of an exchange between Na^+ ions in solution with the H^+ of BAS. This results in a decrease in BAS density of the catalyst. If CBV300 (HY2.6NS) is diffusion limited, the rate (per gram catalyst) should be same for Na+ exchanged HY2.6NS even after a reduction in BAS density of the catalyst. On the other hand, if CBV300 (HY2.6NS) is not diffusion limited, the rate should decrease in proportion with the decrease in BAS density.

Table 6. Comparison of Cracking Rates for CBV300 (HY2.6NS) and Na-CBV300

Zeolite	Weight (mg)	BAS Density (mmol/gm cat)	TOF (hr^{-1})	Rate (mol/hr-gm)	Conversion
CBV300 (HY2.6NS)	50	0.998	3.83 [3.2]	0.0033	5.49 [4.87]
Na-CBV300	50	0.185	7.7 [4.5]	0.0008	2.07 [1.2]

The sodium exchange resulted in about 80% decrease in BAS density. This extensive lowering of BAS might have taken place as every Na^+ has the potential to effectively poison activity equal to 5 framework Al atoms [12, 26]. A subsequent decrease by about 75% for cracking rate can be observed for Na-CBV300 (Na- HY2.6NS) which is an indication that CBV300 (HY2.6NS) is not diffusion limited. The absence of diffusion limitation cannot be strongly proved just on the basis of the observed rate comparisons. Hence, these results from sodium exchange are helpful but not conclusive. This is also because Na^+ exchanged sites might be forming Lewis Acid Sites (LAS) which might influence the activity of the zeolite.

3.4.2 Activity Comparison with 2,3-DMB

In addition to n-hexane cracking, the reaction for cracking of 2,3-DMB was performed. It is a hexane isomer larger in radius than n-hexane molecule. It has 2 tertiary Carbon atoms which makes it easier to crack compared to n-hexane. By comparing the activation energies for cracking of both the molecules on different zeolites (along with their cracking reaction rates), we can have a good idea about diffusion limitations, if any. If a larger molecule is able to enter the pores and react with rates which are greater than or equal to the rates of n-hexane cracking, we can say that the catalysts are not diffusion limited.

For rate calculations, all reaction conditions were kept the same as for n-hexane cracking, except for the reaction temperature. Temperature was lowered down to 400^{o}C because conversions about 3 times higher than n-hexane conversions were observed at 450^{o}C. With increasing conversion, the contribution of secondary reactions towards the products increase [28], which would affect the rate. Hence, lower conversions were

chosen to compare rates, with lower contribution of secondary reactions toward the rate of reaction.

Arrhenius Equation: $\mathbf{k = Ae^{-Ea/RT}}$

Figure 11 shows the Arrhenius Plot, where slope of the plot gives the activation energy. CBV600 (HY2.6St) has the highest rate per gram catalyst as it has a higher mesoporosity compared to CBV300 (HY2.6NS) and higher BAS density compared to CBV760 (HY30).

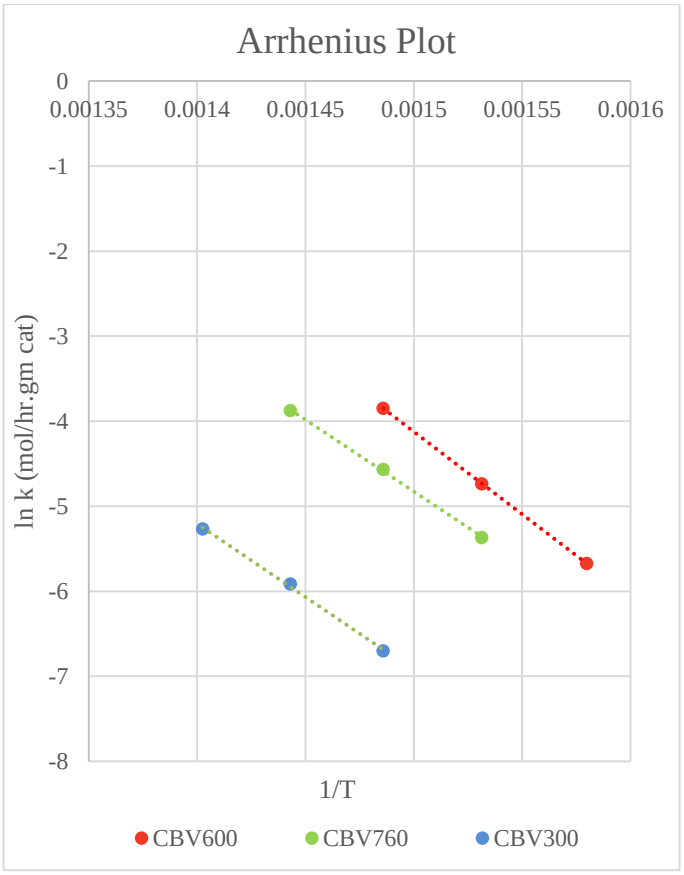

Figure 11. Arrhenius Plot for 2,3 DMB cracking on HY2.6NS, HY2.6St and HY30

As reported in Table 7, the activation energies for 2,3-DMB cracking are higher on all zeolites. At the same time, we see that TOF of cracking is higher for CBV600 (HY2.6St) and CBV760 (HY30) despite of lower temperatures. But, CBV300

(HY2.6NS) has a lower TOF of cracking for 2,3-DMB at 400^{o}C compared to n-hexane cracking at 450^{o}C. Hence, 2,3-DMB cracking was performed at 440^{o}C. The cracking conversion was about 8.5% which was in a good range to compare with conversions obtained for n-hexane cracking at 450^{o}C. The cracking TOF at this temperature was found to be 10.7 molecules/hr which was higher than 3.3 molecules/hr for n-hexane cracking at 450^{o}C. Knowing that catalysts are more active for cracking of a larger molecule, helps us in confirming that the catalysts are not diffusion limited. However, looking at the very low activation energy and low TOF for n-hexane cracking over CBV600 (HY2.6St), possibilities of internal diffusion limitations arise. The possible reasons for internal diffusion limitations for n-hexane cracking over CBV600 (HY2.6St) will be discussed in the later sections of this study.

Table 7. Activation Energy and TOF comparison for cracking of n-hexane and 2,3-DMB, on CBV300 (HY2.6NS), CBV600 (HY2.6St) and CBV760 (HY30)

Zeolites	**Activation Energy (kcal/mol)**		**TOF cracking (hr^{-1})**	
	n-hexane	**2,3-DMB**	**n-hexane (T =450^{o}C)**	**2,3-DMB (T =400^{o}C)**
CBV300 (HY2.6NS)	31.3	34.2	3.3	2.6
CBV600 (HY2.6St)	22.4	38.6	17.9	44.3
CBV760 (HY30)	31.3	33.5	33	43.7

3.4.3 n-hexane cracking over HZSM-5

HZSM-5 was selected for this analysis because small alkane cracking has already been studied by various groups [26, 27] on HZSM-5 catalysts. For this study CBV8014 (HZSM-5) from Zeolyst International was chosen, having a Si/Al ratio of 40. This ZSM-5 has a high Si/Al ratio with Al mostly present in the framework (without

any EFAl). This ensured that the rates obtained would be only on the basis of BAS present inside the framework and only molecules which entered the pores will react.

CBV8014 (HZSM-5) was calcined at 600^{o}C for 5 hours in order to obtain its Proton (H^{+}) form. All the reaction conditions were kept the same and the first reaction was performed with 50 mg of catalyst. The catalyst was used in the form of pellets of size range 90-250 μm. A 100% conversion was obtained for n-hexane cracking over 50 mg of CBV8014 (HZSM-5). Hence, the catalyst weight was lowered down to 30 mg in order to avoid having excess catalyst. It can be seen from Table 8, that TOFs for all the HY zeolites are smaller than the TOF for HZSM-5, although the pores are wider. This is in fair agreement with results in literature [28, 29], therefore it is reasonable to infer that the HY zeolites are not affected by diffusion limitations.

Table 8. Rate Comparison between commercial HY and HZSM-5 Zeolites for n-hexane cracking

Zeolite	BAS Density (mmol/gm catalyst)	TOF (hr^{-1})	TOF cracking (hr^{-1})	Cracking Rate (mol/hr-gm)
CBV300 (HY2.6NS)	0.998	3.83	3.2	0.003
CBV600 (HY2.6St)	0.48	19.5	17.9	0.008
CBV760 (HY30)	0.257	35.51	33	0.008
CBV8014 (HZSM-5)	0.396	78.8	77.1	0.03

3.5 Isolated FAl Effect

The cracking of n-hexane is an established probe for strong acidity in HY zeolites. The structural dealumination of Y zeolites by hydrothermal or chemical treatment is accompanied by enhancement in activity. This activity has been attributed to the generation of stronger BAS, in the form of FAl that has no next nearest neighbor (NNN) Al atom in the framework [7]. Studies by Sohn et. al [7] showed that there is a linear relationship between n-hexane cracking activity and the number of FAl/uc, over the range of 0.7-34 Al/uc. The TOF for n-hexane cracking remained the same in this range of FAl/uc. The same TOF indicated that the strength of all isolated BAS is the same. The cracking activity dropped beyond 34 FAl/uc, which indicates a reduction in the strength of BAS because of increased NNN Al atoms. These results were supported with calculations done by Beagley et. Al [31]. Computational procedures were used to simulate Aluminum distribution in faujasite frameworks. The calculations showed that the number of isolated FAl atoms increases until a maximum of 30 FAl/uc and starts decreasing linearly until it is zero at 64 FAl/uc. The reason for a reduction in BAS strength is postulated to be electrostatic.

Table 5 shows that the activity increases about 4-5 times from CBV300 (HY2.6NS) to CBV600 (HY2.6St). Table 2 shows that CBV300 (HY2.6NS) has 50 FAl/uc, whereas CBV600 (HY2.6St) has about 12.5 FAl/uc which might be an indication of the role of isolated Al atoms towards increasing the activity of the steam dealuminated CBV600 (HY2.6St). To check if the postulated theory can be extended to our results, we can use ^{29}Si MAS NMR spectra. The peaks for Si(1Al) correspond to isolated FAl, whereas the Si(2Al) and Si(3Al) peaks are for Al atoms with no next

nearest neighbor. The percentage peak areas for all three are reported in Table 9. CBV300 (HY2.6NS) show a high amount of non-isolated FAl compared to HY2.6St and HY30, but it also had more isolated FAl. Hence, the role of isolated FAl towards activity enhancement cannot be justified. Therefore, we have to further analyze for reasons leading to activity enhancement in the dealuminated Y zeolites.

Table 9. Percent peak areas occupied by isolated and non-isolated FAl on basis of ^{29}Si MAS NMR spectra

Zeolite	%Peak area				Total %area of Si(2Al) & Si(3Al)
	Si(0Al)	Si(1Al)	Si(2Al)	Si(3Al)	
CBV300 (HY2.6NS)	19.9	32.4	36.9	10.6	47.5
CBV600 (HY2.6St)	90.8	5.6	2.6	0.9	3.5
CBV760 (HY30)	91.25	8.75	-	-	-

3.6 Role of EFAl in Activity Enhancement

The cracking of n-hexane requires presence of BAS in the zeolite, and number of BAS depends on the number of FAl atoms. In the previous section we saw that just isolation of FAl atoms does not help in increasing the cracking activity. Lunsford and co-workers found that the presence of isolated framework Al atoms are necessary but insufficient condition for strong acidity, and only about one-fifth of the framework Al atoms are associated with this strong acidity [12]. A model for strong Brønsted acidity was proposed, consisting of a combination of isolated FAl atoms and a cationic aluminum species residing in the β-cages as $Al(OH)^{2+}$. Inductive effects between this ion and structural OH groups associated with FAl atoms are responsible for their enhanced Brønsted acidity [12, 32].

3.6.1 Combined Effect of FAl and EFAl

There have been various discussions based on a variety of results obtained by different groups, over the role of EFAl in enhancement of cracking activity. Out of those discussions, the synergism between BAS and LAS (generally attributed with EFAl) has been more extensively studied [33, 34, 35]. In studies previously performed in our group by Anh T. To [9] and Yen Pham, it was proposed that synergistic sites are formed due to the interaction between BAS and LAS (formed by the dihydroxylation of EFAl). These studies were done for 2,3-DMB cracking. It would be interesting to compare the n-hexane cracking activity between the steamed and acid leached HY zeolites with different amount of FAl and EFAl.

CBV720 (HY15) and CBV760 (HY30) are prepared by mild acid leaching of the steamed HY zeolite. From Table 10, we see that the FAl/uc values for CBV720 (HY15) and CBV760 (HY30) are similar, but with different EFAl/uc. Also, the ^{27}Al MAS NMR signals show similar types of peaks for Tetrahedral and Octahedral Al. From ^{29}Si MAS NMR spectra it can be inferred that both zeolites have isolated FAl because only Si(0Al) and Si(1Al) peaks were observed. Hence, the possibility of difference in acid strength due to next nearest neighbor Al also can be ruled out. Here, CBV720 (HY15) shows a higher TOF of cracking. Therefore, it can be said that there is a possible effect of EFAl in the cracking activity enhancement. To analyze the possible combined effect of FAl and EFAl in cracking of n-hexane, EFAl/FAl per unit cell ratios were calculated. The cracking activity appears to be a function of the EFAl/FAl ratios for CBV720 (HY15), CBV760 (HY30) and CBV780 (HY40) with CBV720 (HY15) exhibiting the highest TOF of cracking. These results agree with DFT calculation

results observed by Pidko et al. [43] for Protolytic Propane cracking. It was observed that the EFAl present in the inaccessible sodalite cages co-ordinate favorably with supercage BAS and help in activity enhancement [43]. This trend cannot be applied to CBV600 (HY2.6St) because it surely has a very high amount of EFAl, but a large portion of it might be inactive as it might be playing a role of blocking the pores by hindering the internal diffusion of reactants. Another noticeable difference is the TOF of CBV780 (HY40) which has a high amount of isomerization products. CBV780 (HY40) has low FAl as well as EFAl. It has a collapsed structure because of the second steam treatment at very high temperatures. The distances between EFAl and FAl may be very large to have electrostatic interactions, which leads to EFAl acting as LAS. These LAS can add to activity by doing isomerization.

Table 10. Properties and Activities of Commercial Zeolites having EFAl

Zeolites	**FAl/uc**	**EFAl/uc**	**TOF (hr-)**	**TOF of Cracking (hr^{-1})**	**EFAl/FAl per uc**
CBV600 (HY2.6St)	12.5	52.6	19.5	17.9	4.27
CBV720 (HY15)	5.0	6.5	44.1	42.4	1.3
CBV760 (HY30)	4.5	2.2	35.51	33	0.48
CBV780 (HY40)	3.7	1	30.6	21.1	0.27

3.6.2 Removal of Inactive EFAl

We have seen in the previous section that CBV600 (HY2.6St) exhibits lower activity than expected because of inactive EFAl. The pentahedral (or distorted

tetrahedral) EFAl might be the inactive species. A 0.2M HCl solution was used to acid wash CBV600 (HY2.6St) at 80^{o}C. A subsequent washing of EFAl takes place, which is reflected by approximately three times increase in activity when compared to parent CBV600 (HY2.6St). The TOF and conversion values are mentioned in Table 11. The ^{27}Al MAS NMR spectrum (Figure 12) shows no peak for the penta-coordinated EFAl (distorted tetrahedral EFAl). Values reported in Table 11 show a three times increase in TOF of cracking for 0.2MHCl-HY2.6St when compared to its parent HY2.6St. This is an indication of the possible blocking effect of penta-coordinated EFAl.

Table 11. Comparison of HCl washed HY2.6St with Parent HY2.6St at 450^{o}C

Zeolites	**Weight (mg)**	**BAS (mmol/gm.cat)**	**Cracking Conversion (%)**	**TOF (hr^{-1})**	**TOF of Cracking (hr^{-1})**
CBV600 (HY2.6St)	50	0.48	12.5	19.5	17.9
0.2MHCl-CBV600 (0.2MHCl-HY2.6St)	50	0.42	35.2	58.9	58.2

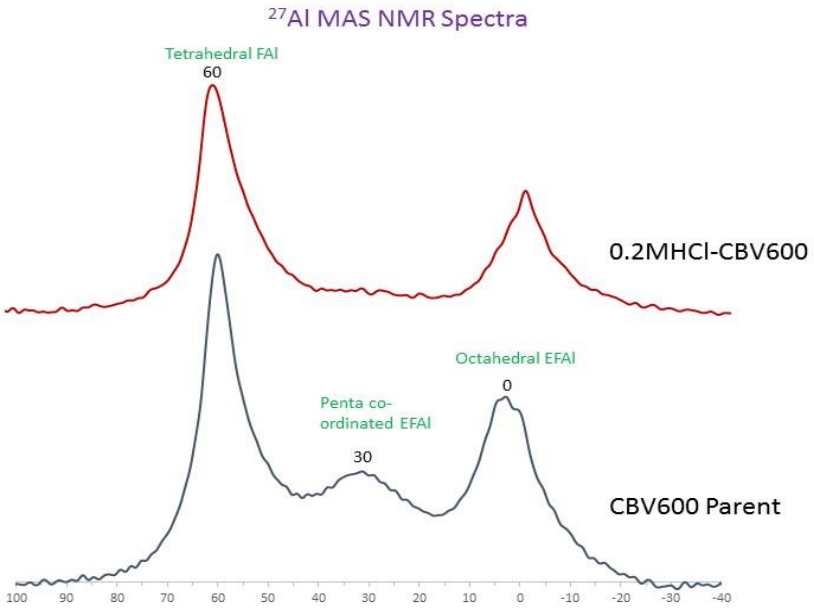

Figure 12. ^{27}Al MAS NMR spectrum of 0.2M HCl acid leached HY2.6St and Parent HY2.6St

3.7 Reaction Mechanism and Product Distribution

We have introduced the different reaction pathways for hexane cracking over HY zeolites in Section 1.4, as depicted in Scheme 2. The monomolecular and bimolecular mechanisms for cracking of alkanes have been proposed and well defined in the past studies [27, 37]. In addition, there has been a refinement to these classifications by defining oligomeric cracking in order to explicitly account for coke and the formation of the products with greater carbon number than the feed [36]. But, in our studies, we will be considering only the first two major mechanisms because products higher than C_6 are not observed in reactions on any of the catalysts used.

3.7.1 Monomolecular Cracking

This mechanism is initiated by protonation of an alkane to form a high energy transition state resembling a strongly surface-coordinated, non-classical, penta-coordinated carbonium ion [27]. It outlines the slow initiation steps for cracking of an alkane after coming in contact with a clean zeolite surface. The activation energy is expected to be high because of the transition state [36]. DFT calculations have shown that protolytic cracking involves an early transition state, which means, it resembles the initial state [38]. On the contrary, dehydrogenation proceeds via formation of a late transition state resembling the final products, which means, the dihydrogen (H_2) molecular part has almost formed and is loose [38]. The late transition state will have a higher entropy compared to the early one because it is a looser species and can have more possible orientations. Looser species are believed to have a higher enthalpy barrier [27]. Therefore, reactions involving looser transition states are more sensitive to the entropic effects, such as Van der Waal's interaction with pore walls and surrounding environment [13].

3.7.2 Bimolecular Cracking

This mechanism involves the chain process of a hydride transfer (H-transfer) step between the reactant gas phase alkane molecule and an adsorbed carbenium ion. The carbenium ion formed through dehydrogenation or protolytic cracking can either isomerize and/or crack, hence keeping the reaction chain going [37]. Once initiated, this pathway is considered to be much faster than the monomolecular reactions [36]. Hence, it also has a lower activation energy and is favored at lower temperatures, higher reactant partial pressures, with higher carbenium ion surface coverage at higher

conversions [27]. There are high possibilities that before the H-transfer to the linear carbenium ion, isomerization and/or β-scission take place which leads to the formation of iso-alkanes through H-transfer. Owing to the high instability of the primary carbenium ion, a hydride shift keeps on taking place in order to attain a stable secondary or tertiary position. Consequent β-scission after the isomerization and hydride shift leads to the formation of a high amount of branched products. Figure 13 shows an example of how iso-alkanes or iso-alkenes can be formed through carbenium ions or a surface hydrocarbon pool.

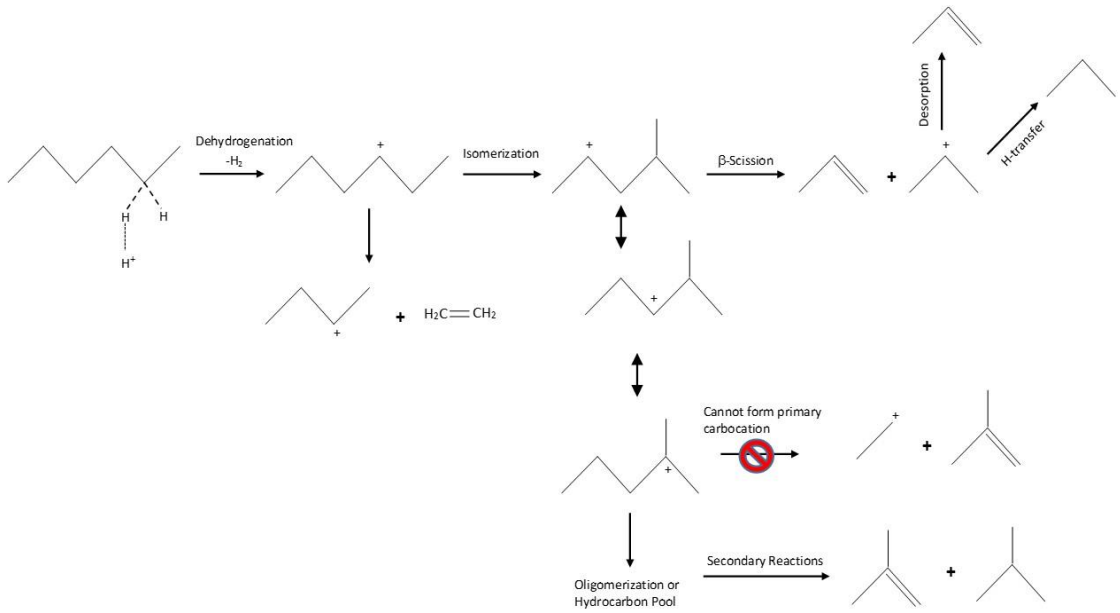

Figure 13. An example of how Primary Carbenium Ion formation is avoided due to instability

3.7.3 Product Distribution for n-hexane Cracking

It has been widely accepted in the literature that the monomolecular and bimolecular pathways always co-exist in the cracking of alkanes [11, 27, 28, 37]. The product distribution will depend on the relative contribution of protolytic and β-scission mechanisms of C–C bond rupture. If bimolecular β-scission mechanism dominates, high yields of branched products will be obtained. In contrast, if protolytic cracking dominates, then more linear paraffins like methane, ethane and also some olefins like ethylene and propylene will be produced. Ideally, if all products were obtained only through monomolecular protolytic cracking, the ratios of $H_2/C_6^=$, C_1/C_5, C_2/C_4, and $C_3/C_3^=$ should be unity. But, as discussed in the earlier section, the reactions involving carbenium ions contribute because of the faster rates and lower activation energies. All these results and discussions from literature can be referred in order to make connection with our results for n-hexane cracking on HY zeolites.

The dealuminated HY zeolites have been of high interest for cracking activity studies. Hence, we selected CBV600 (HY2.6ST) and CBV760 (HY30) for comparison in product distribution, as the former is synthesized by steam dealumination and the latter by mild acid leaching of CBV600. This will also help in knowing changes in product distribution due to difference in synthesis methods, and may be helpful in knowing the role of EFAl in changing the product distribution. The selectivity plots (Figures 14-17) were made for varying conversion points at 450^{o}C by keeping feed concentration constant for all the points. Conversions were varied by varying the weight of catalyst from 10 mg to 65 mg, in such a way that none of the points exceeded 20% conversion on either of the catalysts. This was done to avoid oligomers and other heavy

molecular weight intermediates as much as possible. The conversions and selectivities were calculated for cracking products, i.e. all C_1-C_5 products only. It is worthwhile to mention that the C_6 isomer products seen were very low in both the catalysts, and no products having carbon number greater than 6 were observed. Negligible contribution of Thermal Cracking was observed at 450°C in a test run for n-hexane through flow reactor without any catalyst bed.

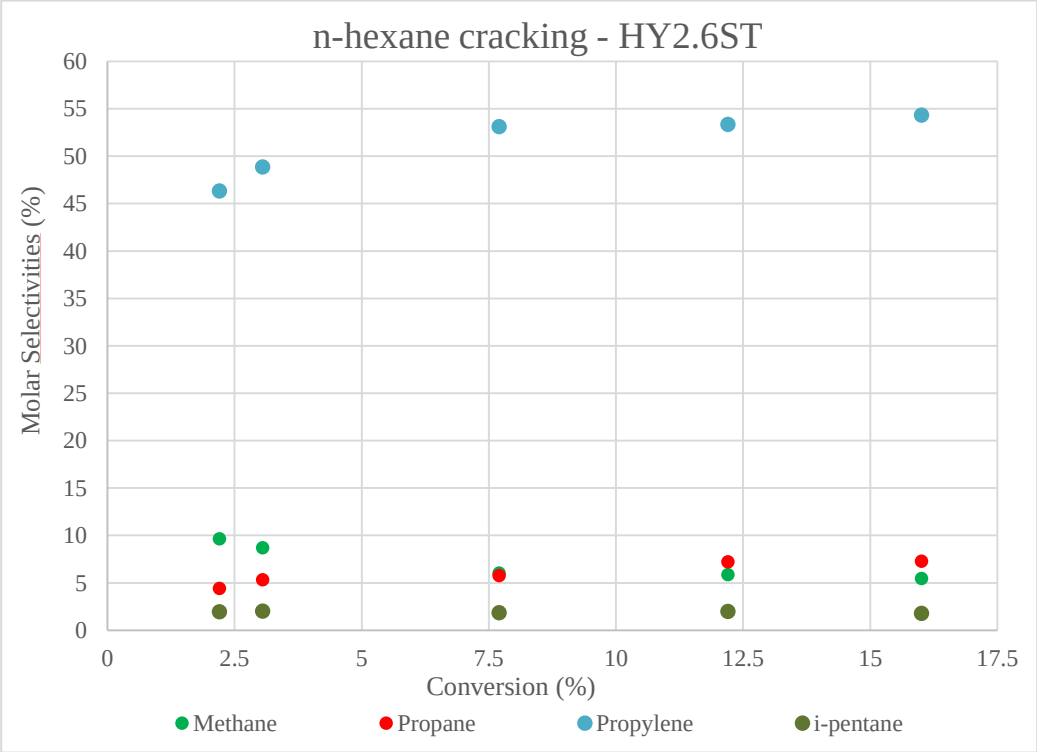

Figure 14. Molar Selectivities for CH_4, C_3H_8, C_3H_6 and i-pentane over HY2.6St

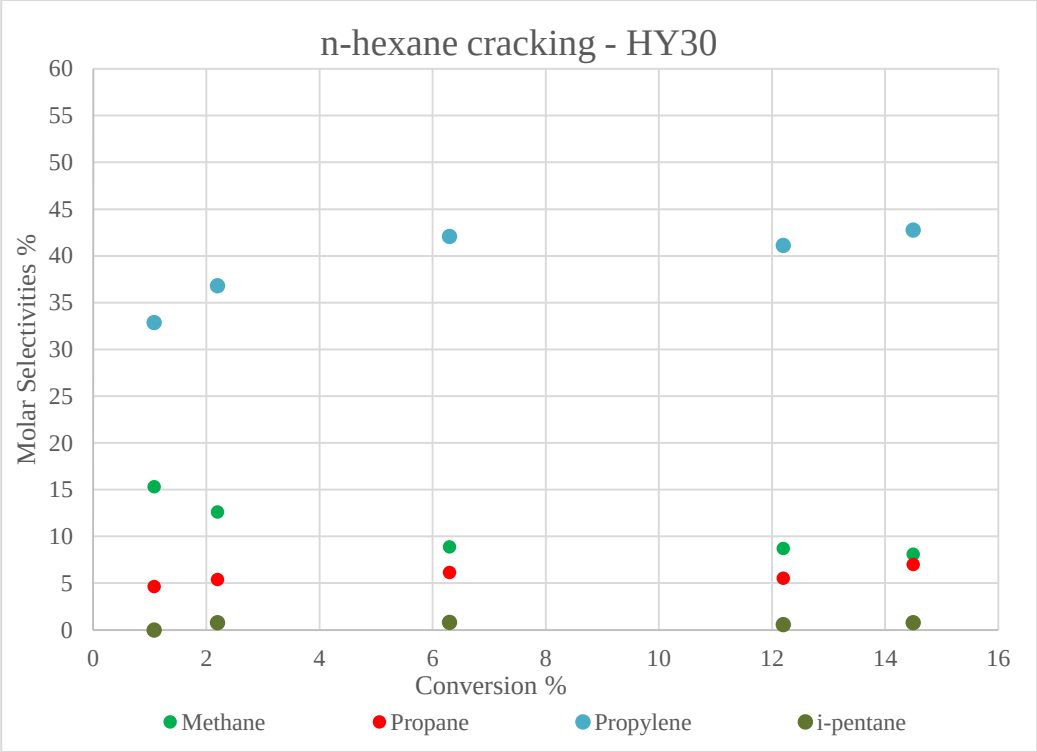

Figure 15. Molar Selectivities for CH_4, C_3H_8, C_3H_6 and i-pentane over HY30

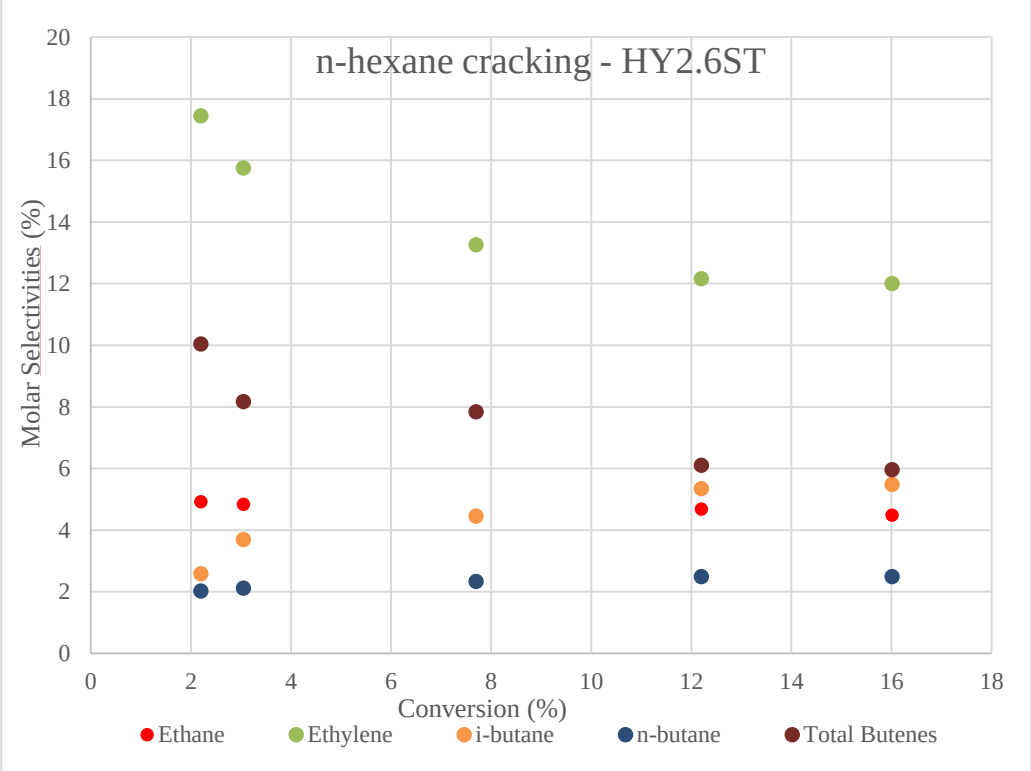

Fig 16. Molar Selectivities for C_2H_6, C_2H_4, i-C_4H_{10}, n-C_4H_{10} & $C4^=$ over HY2.6St

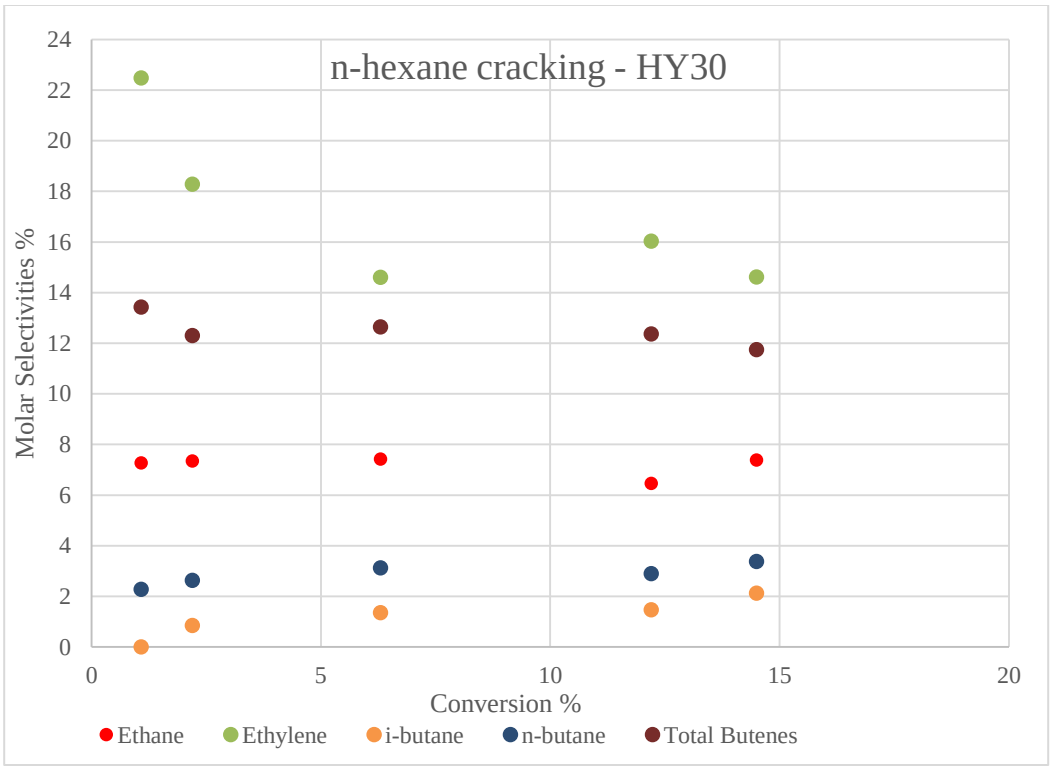

Fig 17. Molar Selectivities for C_2H_6, C_2H_4, i-C_4H_{10}, n-C_4H_{10} & $C4^=$ over HY30

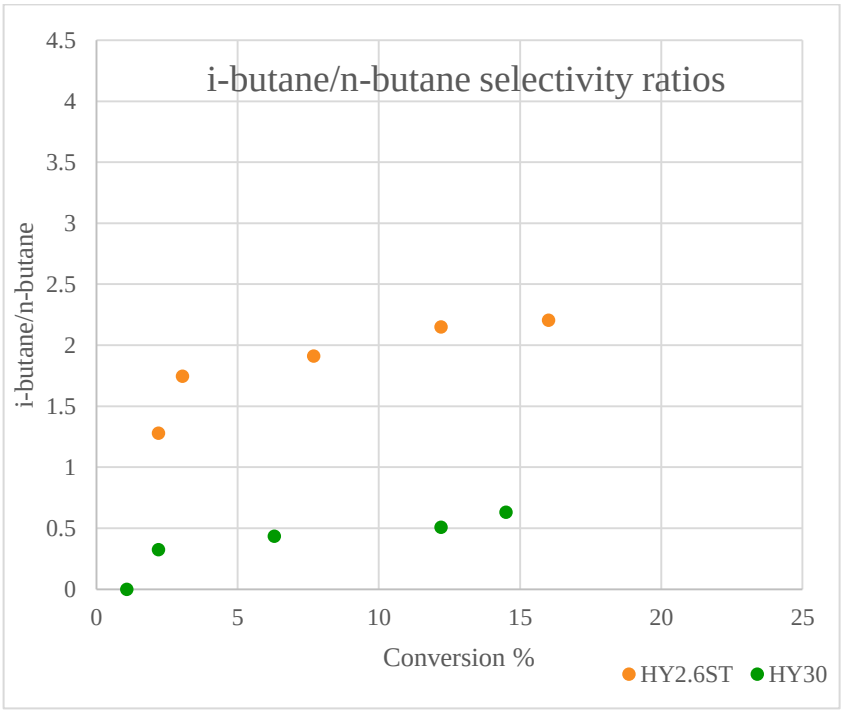

Figure 18. i-butane/n-butane ratios showing contribution of isomerization products for n-hexane cracking over HY2.6St and HY30 at 450°C

From selectivities in Figures 14-17, it can be inferred that the contribution of secondary reactions increases with increasing conversion. Propylene can be formed through multiple pathways in both the mechanisms. Understandably, propylene is the most dominant product and also increases with increasing contribution of secondary reactions for both zeolites. Ethylene is also primarily formed through protolytic cracking. Henceforth, the decrease in Ethylene is seen with increasing conversion. Methane and Ethane cannot be obtained from any of the bimolecular cracking pathways because of the unstable nature of the primary carbocation. Whereas iso-butane is obtained only through isomerization and β-scission, hence it is a good indicator of secondary reactions. From the curves plotted in Figure 18, for iso-butane to n-butane ratios, it can be interpreted that CBV600 (HY2.6St) has more dominant effect of secondary reactions, as selectivity towards iso-butane is higher (at any given conversion) for CBV600 (HY2.6St). From the earlier discussions, we know that Methane and Ethane are obtained just from Protolytic cracking and iso-butane is a characteristic isomerization (followed by β-scission) product; therefore, plotting iso-butane to (Methane + Ethane) ratios would be very helpful in quantifying the relative contributions of the protolytic cracking and β-scission cracking routes [11]. Figure 19 helps in concluding that secondary reactions are majorly responsible for the conversion on CBV600 (HY2.6St), compared to that on CBV760 (HY30). Irrespective of the criterion used, it is widely accepted in literature that the reaction conditions determine the dominating mechanism or pathway [19, 20, 28, 37]. That is, the monomolecular pathway is favored at high reaction temperatures, low paraffin concentrations, and low conversions with low olefin product concentration. In contrast, the bimolecular hydride

transfer reaction is favored at lower reaction temperatures with high paraffin and olefin product concentration [11]. On the contrary, all the reaction conditions in our study are exactly the same for reactions conducted on both the catalysts. Therefore, there are other reasons for this notable difference seen in reaction pathways between CBV600 (HY2.6St) and CBV760 (HY30). We know from earlier reported BET analysis values that CBV600 (HY2.6St) has lower mesopores, whereas CBV760 (HY30) is highly mesoporous because it has undergone acid leaching that leads to a collapse in the structure to form mesopores. This results in a longer diffusion pathway for the products to diffuse out of the zeolite pores, and in turn increases the possibilities of the products getting re-adsorbed on the surface to further isomerize or oligomerize.

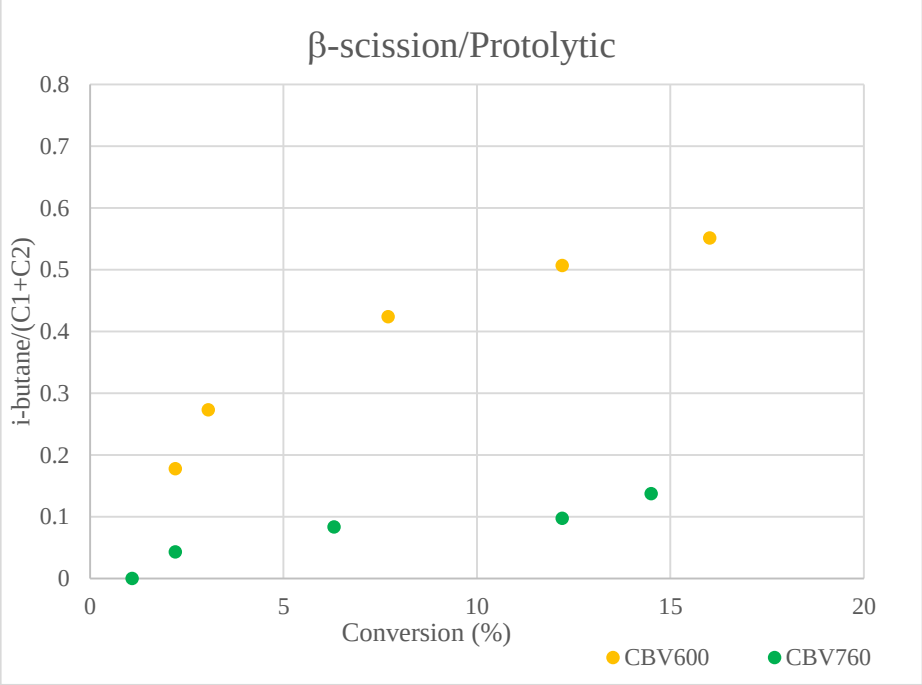

Figure 19. i-butane/(C1+C2) ratios showing contribution of secondary products for n-hexane cracking over HY2.6St and HY30 at 450°C

3.8 Conclusions and Future Work

A detailed study of diffusion limitations was concluded with no limitations observed for n-hexane in entering the pores of HY zeolites. A consequent decrease in the rate on sodium exchanged HY zeolite because of a reduced BAS density was observed. In addition, an increase in the TOF of cracking for 2,3-DMB cracking was seen, which is a larger molecule compared to n-hexane, but at the same time is easier to crack. HZSM-5 had a considerably high TOF of cracking when compared to any other HY zeolites used in this study. The discussed three results, were collectively conclusive of the absence of diffusion limitations of the reactant through the pore entrance of the HY zeolites. The major reason being that the pore diameter in HZSM-5 is smaller than the HY supercages. However, the comparison of apparent activation energies for CBV300 (HY2.6NS), CBV600 (HY2.6St) and CBV760 (HY30) reflected a decrease in CBV600 (HY2.6St) by 6-8 kcal/mol. This could possibly have been because of the penta co-ordinated EFAl blocking the diffusion of molecules through the pore channels, which was observed only in case of CBV600 (HY2.6St). This explanation could be backed up with the results seen in 0.2MHCl-CBV600 (0.2MHCl-HY2.6St), where the activity increased two folds after the penta co-ordinated EFAl was washed away by acid treatment without modifying BAS density much.

The study of isolated FAl showed no particular trend in the activity of different commercial HY zeolites. But, the activity of zeolites linearly increased with increasing EFAl/FAl ratio. CBV600 (HY2.6St) did not follow this trend as it was thought to have excess of EFAl, and also a lot of it in the distorted tetrahedral or

penta co-ordinated positions. Rather, this meant that the BAS (FAl) to LAS (EFAl) co-ordination (for activity enhancement) is also dependent on the position and type of EFAl present in the zeolite.

The product distribution comparison between CBV600 (HY2.6St) and CBV760 (HY30) clearly showed that the cracking of n-hexane is taking place through a concerted mechanism between monomolecular and bimolecular pathways. Propylene was found to be the most abundant product in both the catalysts as it can be obtained from multiple paths. The secondary products increase with increasing conversion even at the same temperature. The different selectivity ratios plotted with respect to iso-butane showed that the secondary reactions are dominant more in CBV600 (HY2.6St), than in CBV760 (HY30). This is because of the longer diffusion path in CBV600 (HY2.6St), which increases the possibility of the re-absorption of products before they diffuse out of the zeolites pores resulting in an increased possibility of isomerization and oligomerization.

It would be very important in knowing the role of EFAl depending on its position in the zeolite. Hence, EFAl can be impregnated in the CBV300 (HY2.6NS), which has very low or negligible EFAl. The NMR characterization can show the Al positions in the zeolite. This study would serve two purposes: (1) In understanding the position-wise role of EFAl in co-ordination with FAl. (2) If the activity of the EFAl impregnated CBV300 (HY2.6NS) increases by a very high number then it can be said that isolated FAl is not required for creating stronger BAS. Instead, an interaction between FAl and EFAl is important in creating more active BAS.

To exactly know about the dominant reaction mechanism (monomolecular or bimolecular) in the different HY zeolites, iso-butane can be used as a probe molecule. Methane and propylene would be the only protolytic cracking products. Presence of a high amount of other products would strongly show the dominance of secondary reactions in the particular zeolites.

References

[1] T. Chiranjeevi, N. Ravichander, D. T. Gokak, V. Ravikumar, N. V. Choudary, Petroleum Science and Technology, 470 – 478 (2014) 32.

[2] R. Sadeghbeigi, Fluidized Catalytic Cracking handbook, 2nd Ed., Gulf Professional Publishing, 2000.

[3] Geldart, G., "Challenges in Fluidized Bed Technology," AIChE Symposium Series No. 270, 85, p. 111, 1989.

[4] Lu Zhang, Kuizhi Chen, Banghao Chen, Jeffery L. White, Daniel E. Resasco; J.Am.Chem. Soc. 2015, 137, 11810−11819

[5] Zeolite Y: Synthesis, Modification, and Properties—A Case Revisited Wolfgang Lutz

[6] J. Weitkamp, Solid State Ionics, 175 – 188 (2000) 131.

[7] J. R. Sohn, S. J. DeCanio, P. O. Fritz, J. H. Lunsford, J. Phys. Chem., 4847 (1986) 90.

[8] R. A. Beyerlein, G. B. McVicker, L. N. Yacullo, J. J. Ziemiak, J. Phys. Chem., 1967 (1988) 92.

[9] Anh T. To, Rolf E. Jentoft, Walter E. Alvarez, Steven P. Crossley, Daniel E. Resasco, Journal of Catalysis 317 (2014) 11–21

[10] Marios S. Katsiotis, Michael Fardis, Yasser Al Wahedi, J. Phys. Chem. C 2015, 119, 3428−3438

[11] A.T. To, D.E. Resasco / Journal of Catalysis 329 (2015) 57–68

[12] P. 0. Fritz and J. H. Lunsford, J. Catal., 1989, 118, 85.

[13] Rajamani Gounder and Enrique Iglesia/ *Chem. Commun.,* 2013, **49**, 3491—3509

[14] D. C. Tranca, P. M. Zimmerman, J. Gomes, D. Lambrecht, F. J. Keil, M. Head Gordon, and A. T. Bell, J. Phys. Chem. C 2015, 119, 28836−28853

[15] F.L. Raúl, Introduction to the Structural Chemistry of Zeolites, in: Handbook of Zeolite Science and Technology, CRC Press, 2003.

[16] O. M. L. Occelli, P. O' Connor, in: Fluid Catalytic Cracking V: Materials and Technological Innovations, Studies in Surface Science and Catalysis, Vol. 134, Elsevier, 2001.

[17] S. Bordiga, P. Ugliengo, A. Damin, C. Lamberti, G. Spoto, A. Zecchina, G. Spano, R. Buzzoni, L. Dalloro, F. Rivetti, Top. Catal. 15 (2001) 43.

[18] R. D. Shannon, K. H. Gardner, R. H. Staley, G. Bergeret, P. Gallezot, A. Auroux, J. Phys. Chem., 89 (1985) 4778

[19] J. Abbot, J. Catal. 126 (1990) 628.

[20] W.O. Haag, R.M. Dessau, R.M. Lago, Stud. Surf. Sci. Catal. 60 (1991) 255.

[21] R. D. Shannon, K. H. Gardner, R. H. Staley, G. Bergeret, P. Gallezot, A. Auroux, J. Phys. Chem., 89 (1985) 4778.

[22] J. Klinowski, S. Ramdas, J. M. Thomas. J. Chem. Soc., Faraday Trans. 2, 78 (1982)1025.

[23] J. R. Sohn, S. J. DeCanio, J. H. Lunsford, D. J O'Donnell, Zeolites, 6 (1986) 225.

[24] Prasad V. Shertukde, George Marcel1n, Gustave A. Sill, W. Keith Hall, Journal of catalysis 136,446-462(1992)

[25] Eduardo A. Lombardo, W. Keith Hall Journal of Catalysis 112, 565-578 (1988)

[26] H. Krannila,W.O. Haag, B.C. Gates, J. Catal. 135 (1992) 115.

[27] W.O. Haag, R.M. Dessau, in: Proceedings of the Eighth International Congress on Catalysis, vol. II, Verlag Chemie, Weinheim, Berlin, 1984, p. 305.

[28] S.M. Babitz et al. / Applied Catalysis A: General 179 (1999) 71-86.

[29] W.O. Haag, R.M. Lago, P.B. Weisz, Faraday Disc. Chem. Soc. 72 (1981) 317.

[30] Nigel P. Rhodes, Robert Rudham and Nicholas H. J. Stanbridge, *J. Chem. Soc., Faraday Trans.*, 1996, **92**, 2817-2823

[31] B. Beagley, J. Dwyer, F. Fitch, R. Mann, J. Walters, J. Phys. Chem., 88 (1984) 1744.

[32] R. Carvajal, P-J. Chu and J. H. Lunsford, J. Catal., 1990, 125, 123

[33] Mirodatos, C.; Barthomeuf, D. J. Chem. Soc., Chem. Commun. 1981, 2, 39-40.

[34] Wang, Q. L.; Giannetto, G.; Guisnet, M. J. Catal. 1991, 130, 471-482.

[35] Corma, A.; Forne´s, V.; Rey, F. Appl. Catal. 1990, 59, 267-274.

[36] B.A. Williams, S.M. Babitz, J.T. Miller, R.Q. Snurr, H.H. Kung, Applied Catalysis A: General 177 (1999) 161-175

[37] A. Corma, A.V. Orchillés, Microporous Mesoporous Mater., 35–36 (2000) 21.

[38] S. Mallikarjun Sharada, P.M. Zimmerman, A.T. Bell, M. Head-Gordon, The Journal of Physical Chemistry C, (2013).

[39] S.T. Sie, Ind. Eng. Chem. Res. 31 (1992) 1881

[40] Mota, C. J. A.; Bhering, D. L.; Rosenbach, N. Angew. Chem., Int. Ed. 2004, 43, 3050−3053.

[41] S. Li, A. Zheng, Y. Su, H. Zhang, L. Chen, J. Yang, C. Ye, F. Deng, J. Am. Chem. Soc., 129 (2007) 11161.

[42] David S.J. Jones and Peter P. Pujado (Editors) (2006). *Handbook of Petroleum Processing* (First ed.). Springer.

[43] Chong Liu, Guanna Li, Emiel J. M. Hensen, and Evgeny A. Pidko, ACS Catal. 2015, 5, 7024−7033

[44] Elements of Chemical Reaction Engineering, Fourth Edition, H. Scott Fogler, Chapter 10

[45] Davis, Mark E. and Davis, Robert J. (2003) *Fundamentals of chemical reaction engineering.* McGraw-Hill Higher, Chapter 6

[46] Chen. N.Y., Garwood, W.E., and Dwyer, F.G., "Shape Selective Catalysis in Industrial Applications" Marcell Dekker, Inc., 1989.

Appendix A: Standard Operation Procedure for Continuous Flow Reactor

Preparation:

- Prepare the reactor tube: pack the catalyst between the glass beads. Catalyst bed height varies depending on the amount and type of catalyst.
- Turn on N_2 flow
- Install reactor tubes into the oven then increase the pressure of the GC FID to 30 psi. Check leaks and cover the oven by ceramic wool.
- Turn on the heating tapes. Set heating capacity on voltage regulator;
- Turn on the furnace. Set the temperature ramp.
- Load and/or adjust GC method, then turn on the air and hydrogen gas flows in order to ignite the flame in FID;
- Adjust GC oven temperature to maximum high temperature (depends on the type of column).
- Fill the syringe with reactant (or reactant mixture) and insert syringe outlet in to injection port. Set pump flow rate and max volume.
- Wait until the system's temperature is stable.

Run reaction:

- Turn on the syringe pump and hit RUN;
- Input information for the GC run;

- After the intended time on stream for product analysis, turn the six-port valve in injection mode for one minute; this will allow the product stream to pass to the column in GC-FID;
- After one minute, turn the six-port valve to vent mode; this will purge all the products to the vent.
- Repeat the above two steps in specified time intervals for product analysis.

Stop reaction:

- - Stop syringe pump;
- - Turn off heating box, heating tapes and oven. Wait for cooling down before turning off N_2 gas flows and dissembling the reactor tubes;
- Load OFF method, turn off air and hydrogen gas flows.

Appendix B: Raw Data

Table 12. Molar Selectivities for Cracking Products over CBV300, CBV600 and CBV760. The reaction temperature was 450ºC.

Products	CBV300	CBV600	CBV760
Methane	8.22	5.88	8.94
Ethane	5.60	4.68	6.63
Ethylene	13.49	12.16	16.44
Propane	5.10	7.23	5.66
Propylene	51.50	53.37	42.17
Total Butanes	4.30	7.84	4.49
Total Butenes	9.01	6.11	12.68
Total Pentanes	1.23	2.09	0.59
Total Pentenes	1.55	0.64	2.41

Table 13. Molar Selectivities at Zero Conversion for Cracking Products over CBV600 and CBV760. The values are calculated from extrapolation of the selectivity curves in Figures 14-17

Products	CBV600	CBV760
Methane	6.2	10.9
Ethane	4.5	6
Ethylene	11.9	15.5
Propane	3.7	3.7
Propylene	41.7	25.3
Iso-butane	2.7	0
n-butanes	1.6	2.2
Total Butenes	7.1	11.1
Total Pentanes	1.9	0.37
Total Pentenes	0.57	2.3

Table 14. FAl and EFAl Quantification with BAS Density and activity for all commercial Zeolites. The reaction was carried out for cracking of n-hexane at 450°C

Zeolites	FAl/uc	EFAl/uc	BAS Density (mmol/gm.cat)	TOF of Cracking (hr^{-1})	Rate (mol/hr.gm)
CBV300	50.1	n/a	0.998	3.2	0.0038
CBV600	12.5	52.6	0.48	17.9	0.0052
CBV720	5.0	6.5	0.356	42.4	0.0152
CBV760	4.5	2.2	0.257	33	0.0084
CBV780	3.7	1	0.09	21.1	0.0027